

Photolytic Activation of Late Transition Metal Carbon Bonds and their Reactivity towards Oxygen

*Sarah K.Y. Ho,^{a)} Francis Y.T. Lam,^{a)} Adiran de Aguirre,^{b)} Feliu Maseras^{b)}, Andrew J.P. White^{a)} and George J.P. Britovsek^{*a)}*

a) Department of Chemistry, Imperial College London, Molecular Sciences Research Hub, White City Campus, 80 Wood Lane, London, W12 0BZ, United Kingdom.

b) Institute of Chemical Research of Catalonia, The Barcelona Institute for Science and Technology, Avgda. Països Catalans, 16, Tarragona 43007, Catalonia, Spain.

Abstract

Photolytic activation of palladium(II) and platinum(II) complexes [M(**BPI**)(R)] (R= alkyl, aryl) featuring the 1,3-bis(2-pyridylimino)isoindole (**BPI**) ligand has been investigated in various solvents. In the absence of oxygen, the formation of chloro complexes [M(**BPI**)Cl] is observed in chlorinated solvents, most likely due to photolytic degradation of the solvent and formation of HCl. The reactivity of the complexes towards oxygen has been studied both experimentally and computationally. Excitation by UV irradiation (365 nm) of the metal complexes [Pt(**BPI**)Me] and [Pd(**BPI**)Me] leads to distortion of the square planar coordination geometry in the excited triplet state and a change in the electronic structure of the complexes that allows the interaction with oxygen. TD-DFT computational studies suggest that in the case of palladium, a Pd(III) superoxide intermediate [Pd(**BPI**)(κ^1 -O₂)Me] is formed and, in the case of platinum, a Pt(IV) peroxide intermediate [Pt(**BPI**)(κ^2 -O₂)Me]. For alkyl complexes where metal carbon bonds are sufficiently weak, the photo-activation leads to the insertion of oxygen into the metal carbon bond to generate alkylperoxo complexes, for example [Pd(**BPI**)OOMe], which has been isolated and structurally characterised. For stronger M–C(aryl) bonds, the reaction of [Pt(**BPI**)Ph] with O₂ and light results in a Pt(IV) complex, tentatively assigned as the peroxo complex [Pt(**BPI**)(κ^2 -O₂)Ph], which in chlorinated solvents reacts further to give [Pt(**BPI**)Cl₂Ph], which has been isolated and characterised by scXRD. Besides facilitating oxygen insertion reactions, UV irradiation can also affect the reactivity of other components in the reaction mixture, such as the solvent or other reaction products, which can result in further reactions. Labelling studies using [Pt(**BPI**)(CD₃)] in chloroform have shown that photolytic reactions with oxygen involve degradation of the solvent.

Introduction

The selective functionalisation of alkanes remains one of the great challenges in catalysis research. The abundant availability of methane and light alkanes from shale gas has led to an increase in natural gas conversion in recent years.¹⁻² Methane conversion is carried out predominantly via steam reforming to syngas, whereas higher alkanes are generally converted to alkenes, for example via ethane cracking or propane dehydrogenation.³⁻⁴ Considerable progress has been made during the last three decades regarding the organometallic activation of alkanes in solution, in particular through electrophilic activation with late transition metals.⁵⁻⁹ Once C-H bond cleavage has been achieved at a metal centre, a functionalisation of the metal carbon bond is required, followed by release of the product and regeneration of the catalyst. In the case of oxidation reactions, this functionalisation of metal alkyl complexes should be carried out ideally with environmentally benign oxidants such as O₂ or H₂O₂, an area of research that has seen a great deal of interest and tremendous advances have been made in recent years.¹⁰⁻¹³

The air-sensitive nature of many organometallic compounds often results in uncontrollable reactions upon exposure to oxygen. The insertion of oxygen into metal carbon bonds (M–R) to give stable peroxo metal complexes (M–OOR) is an intriguing departure from this general reactivity. In the context of catalytic alkane oxidations, oxygen insertions could become particularly important for metals with a track record in C-H activation such as palladium and platinum.¹¹

Oxygen insertion reactions have been reported for a number of transition metal alkyl or aryl complexes, in particular for first row metals like chromium,¹⁴ iron,¹⁵⁻¹⁶ cobalt,¹⁷⁻¹⁹ nickel,²⁰ and zinc.²¹⁻²² During the past decade, several oxygen insertions with palladium(II) and platinum(II) methyl complexes have been reported. In 2009, Goldberg reported the reaction of [(PN)PtMe₂] (PN = 2-(di-tert-butylphosphino)methylpyridine) with oxygen to give a platinum(II) methylperoxo complex [(PN)PtMe(OOMe)],²³ and the formation of a palladium(II) methylperoxo complex [(bipy)PdMe(OOMe)] (bipy = 2,2'-bipyridine) via the reaction of [(bipy)PdMe₂] (bipy = 2,2'-bipyridine) with oxygen (Figure 1).²⁴ A radical initiator (AIBN) was used in these oxygen insertions to activate the metal complexes and kinetic analyses indicated a radical chain mechanism for the oxygen insertion process. Around the same time, we reported the insertion of oxygen with terpyridine platinum and palladium methyl complexes such as [Pt(diaminoterpy)Me]⁺ (diaminoterpy = 6,6''-diaminoterpyridine) to give [Pt((diaminoterpy)OOMe)]⁺.²⁵⁻²⁶ The insertion reaction proceeds at room temperature in

various solvents within minutes in the presence of UV light. Steric repulsion between the substituents at the 6,6''-positions on the terpyridine ligand and the methyl ligand causes a bending of the N(pyr)-Pt-C angle to approximately 167° ,²⁷ which weakens the M-C bond for oxygen insertion. The formation of dinuclear triplet M(III)-M(III) intermediates was proposed upon excitation of the square planar M(II) complexes, which subsequently react with oxygen. Similar oxygen insertion reactions have been reported by Martín and co-workers with dinuclear half-lantern Pt(III) methyl complexes,²⁸ and other dinuclear Pd(III) complexes have also been implicated in reactions with oxygen.²⁹⁻³²

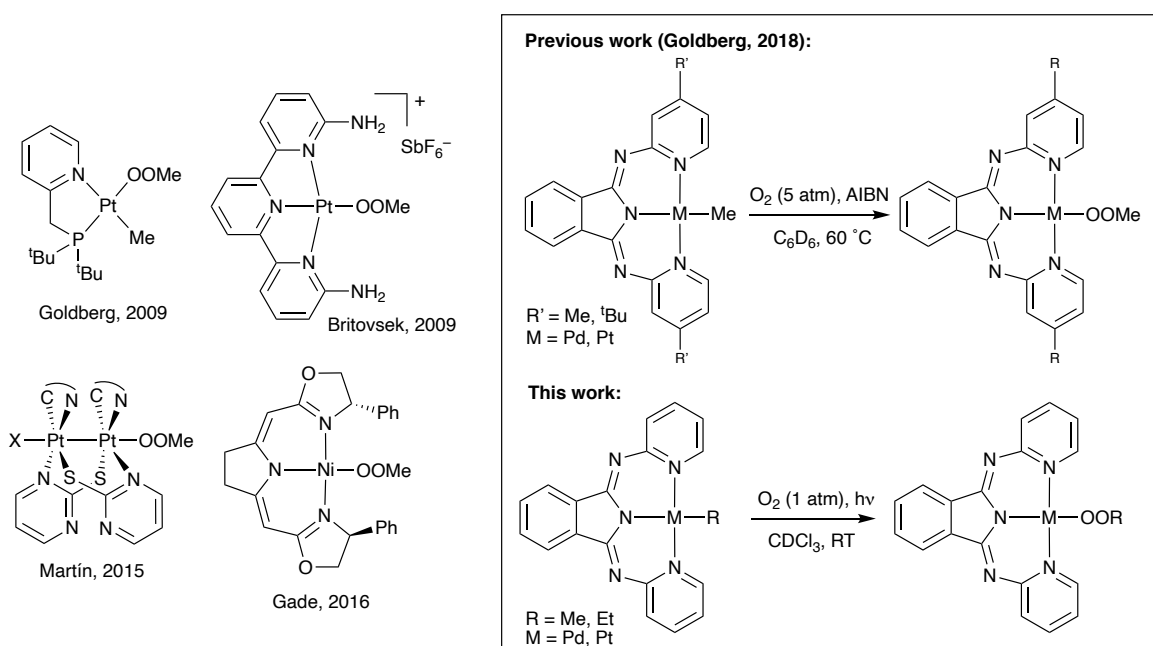


Figure 1. Examples of Group 10 methylperoxo complexes prepared via oxygen insertion reactions.

In search of a monoanionic ligand, similar to terpyridine, that would allow the use of less polar solvents, ideally alkanes, we turned to 1,3-bis(2-pyridylimino)isoindole (BPI). This ligand, first reported in 1952,³³ has a highly delocalised electronic structure, akin to porphyrin and terpyridine ligands. Indeed, the electronic and photophysical properties of Pt(II) and Pd(II) BPI complexes with a range of additional ligands, have been investigated in great detail.³⁴⁻³⁷ Goldberg recently reported the oxygen insertion of Pt(II) and Pd(II) methyl complexes with BPI-type ligands to give methylperoxo complexes (see Figure 1).³⁸ Kinetic studies with AIBN as an initiator indicated a radical chain mechanism for the oxygen insertion process. Noteworthy in this context are also the earlier studies on cobalt(III) alkylperoxy complexes with BPI ligands that have been applied in the photo-induced oxidation of hydrocarbons.³⁹⁻⁴¹

The oxygen insertion with a related nickel(II) methyl complex to give a methylperoxo complex, as shown in Figure 1, is also relevant in this context.⁴²

Here we present an extensive investigation on Pd(II) and Pt(II) BPI complexes with alkyl and aryl ligands and their reactivity towards light and oxygen (see Figure 1). For certain complexes, oxygen insertion is strongly accelerated by light. Electronic excitation through light absorption modifies the electronic and chemical properties of the metal BPI complexes,⁴³ which affects their reactivity towards oxygen. These findings are important for the development of electrophilic late transition metal catalysts for alkane oxidations, and also in the context of the photoluminescent stability of BPI and related metal complexes. During light irradiation, the metal complex is however not the only species affected and other components in the reaction mixture, such as the reaction products and the solvent, can also be affected by light.

Results and discussion

BPI metal complexes

The ¹H NMR spectrum of [Pt(**BPI**)Me] in CDCl₃ shows a diagnostic doublet signal for the protons in 6-position of the pyridine at 9.19 ppm (³J_{Pt-H} = 52 Hz), in addition to a singlet at 1.04 ppm (²J_{Pt-H} = 72 Hz) for the Pt-Me protons (see Supporting Information for synthetic details). The ethyl complex [Pt(**BPI**)Et] has spectroscopic signals for the pyridyl 6-position at 9.21 ppm (³J_{PtH} = 56 Hz) together with the CH₂ protons at 1.69 ppm (²J_{PtH} = 76 Hz) and CH₃ at 1.06 ppm (³J_{PtH} = 36 Hz). In the previously reported phenyl complex [Pt(**BPI**)Ph]⁴⁴, the pyridyl protons at the 6-position appear at 8.64 ppm, approximately 0.5 ppm lower than for the methyl and ethyl complexes, with ¹⁹⁵Pt satellites of ³J_{Pt-H} = 55 Hz. All spectroscopic data are consistent with previously reported data, and complexes [Pt(**BPI**)Me] and [Pt(**BPI**)Ph] were further characterised by scXRD analysis (see Figure 2 and Supporting Information). The palladium complex [Pd(**BPI**)Me] shows the protons at the 6-position of the pyridine moieties at 8.79 ppm as a doublet and the Pd-Me protons as a singlet at 0.77 ppm and this complex was also characterised by scXRD (see Figure 2). Common to all structures [Pt(**BPI**)Me], [Pd(**BPI**)Me] and [Pt(**BPI**)Ph] is that the methyl and phenyl ligands are pushed out of the square coordination plane, with a N-M-C bond angle of 167.3(13)° for complex [Pt(**BPI**)Me], 165.3(4)° for complex [Pd(**BPI**)Me] and 168.82(11)° for [Pt(**BPI**)Ph] (see Figure 2). This distortion is likely due to steric repulsion with the hydrogen atoms at the ortho position of the pyridine rings.

Similar distortions were seen in the recently reported related BPI Pt(II) and Pd(II) methyl complexes by Goldberg.³⁸ Noteworthy, out of plane distortions with N-M-C angles of approximately 167° have been seen previously in our studies on oxygen insertion reactions with 6,6''-disubstituted terpyridine Pt(II) and Pd(II) methyl complexes.²⁶

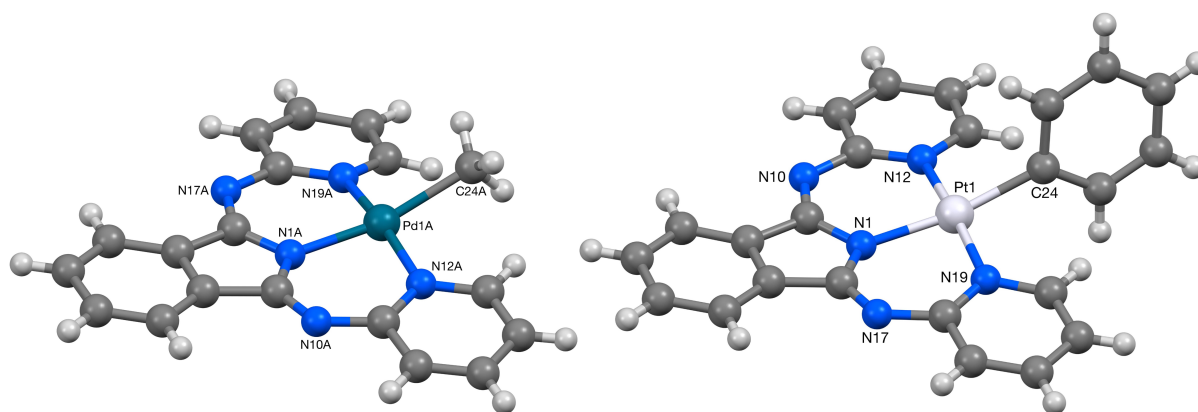


Figure 2. Molecular structures determined by scXRD analysis of complexes $[\text{Pd}(\text{BPI})\text{Me}]$ and $[\text{Pt}(\text{BPI})\text{Ph}]$ showing N1-M-C24 bond angles $<180^\circ$.

Reactivity under UV light irradiation

The stability of the palladium and platinum BPI complexes during irradiation with UV light (365 nm) was investigated first in the absence of oxygen. The electronic spectrum of $[\text{Pt}(\text{BPI})\text{Me}]$ in CDCl_3 shows absorptions between 420 nm to 530 nm, suggesting $[5d(\text{Pt}) \rightarrow \pi^*(\text{BPI})]$ MLCT transitions and the bands around 304 nm and 351 nm are assigned to $[\pi \rightarrow \pi^*(\text{BPI})]$ IL transitions (Figure S39).⁴⁵ After this solution (under nitrogen) was exposed to UV light for 38 hours at room temperature, most starting complex $[\text{Pt}(\text{BPI})\text{Me}]$ remained unreacted according to ^1H NMR spectroscopy, but with 10% (relative to the starting complex) of the chloro complex $[\text{Pt}(\text{BPI})\text{Cl}]$, together with small amounts of CH_4 , CH_3D and CH_3Cl (see Figure S1). The characteristic protons at the 6-position of the pyridine for $[\text{Pt}(\text{BPI})\text{Cl}]$ are at 10.31 ppm ($^3J_{\text{Pt-H}} = 56$ Hz) in CDCl_3 , cf. 9.19 ppm ($^3J_{\text{Pt-H}} = 52$ Hz) for $[\text{Pt}(\text{BPI})\text{Me}]$. When a CDCl_3 solution of $[\text{Pt}(\text{BPI})\text{Me}]$ is kept in the dark for 24 hours, very little ($\sim 1\%$) of the chloro complex is detected, probably due to small amounts of DCl present in CDCl_3 . In $\text{THF-}d_8$, $[\text{Pt}(\text{BPI})\text{Me}]$ is stable in the dark and towards exposure to UV light for 24 hours.

The ethyl complex $[\text{Pt}(\text{BPI})\text{Et}]$ (6-H at 9.22 ppm, $^3J_{\text{Pt-H}} = 52$ Hz) converts after several hours irradiation in CDCl_3 initially to an intermediate with a new set of aromatic signals and the

pyridine 6-H signal at 9.66 ppm ($^3J_{\text{Pt-H}} = 44$ Hz), together with ethane ($\text{C}_2\text{H}_5\text{D}$ with some C_2H_6) and small amounts of ethyl chloride, as shown in Figure 3. There are no other new signals, neither in the ^1H nor in the ^2H NMR spectrum. The intermediate could not be isolated and identified so far, but it is suspected to be a T-shaped cationic $[\text{Pt}(\text{BPI})]^+$ or solvent-stabilised $[\text{Pt}(\text{BPI})(\text{solv})]^+$ complex,⁴⁶ formed upon reaction with DCl , which slowly reacts further to give the chloro complex $[\text{Pt}(\text{BPI})\text{Cl}]$. An alternative possibility is homolytic M-C bond cleavage and formation of a dinuclear Pt(I) complex $[\text{Pt}(\text{BPI})]_2$, analogous to the dinuclear Pd(I) dimer reported by Ozerov and co-workers, which was obtained upon irradiation of a Pd(II) ethyl complex with a monoanionic PNP ligand.⁴⁷ Further irradiation for 20 hours in CDCl_3 at room temperature results in complete conversion to $[\text{Pt}(\text{BPI})\text{Cl}]$ (see Figure 3).

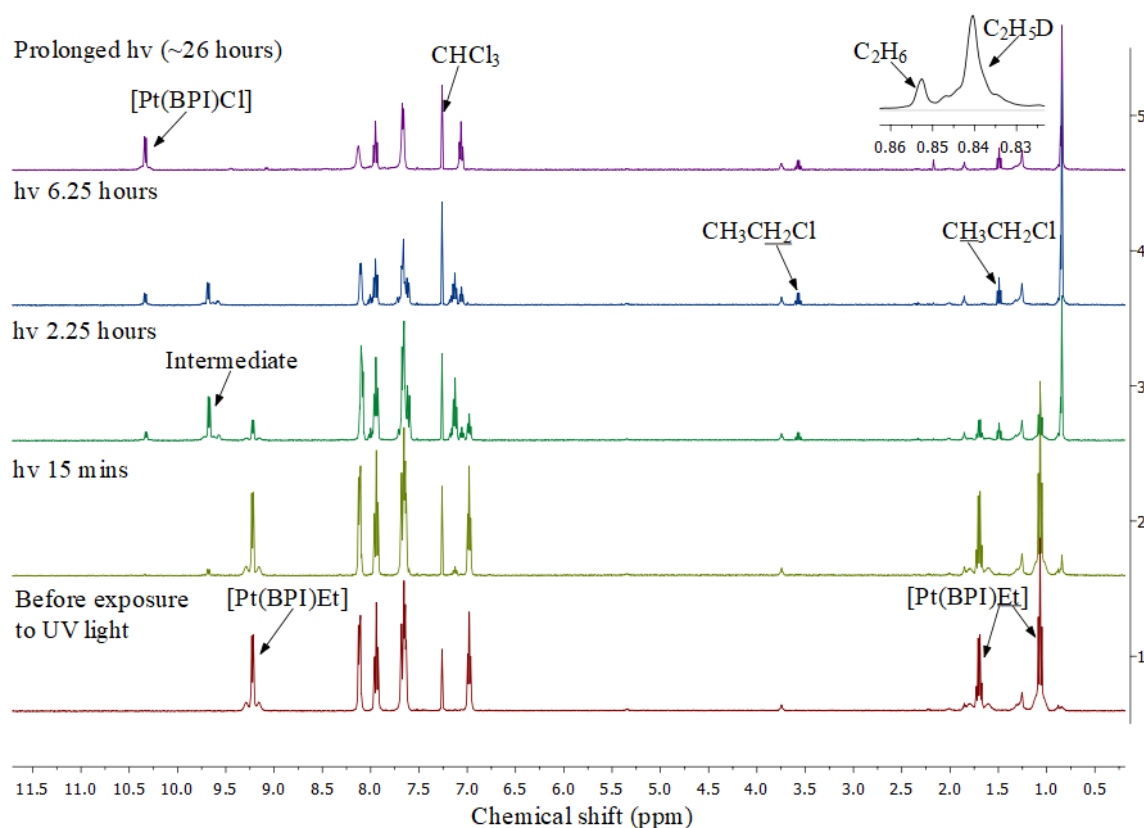


Figure 3. The reaction of $[\text{Pt}(\text{BPI})\text{Et}]$ in CDCl_3 upon irradiation (365 nm) at room temperature.

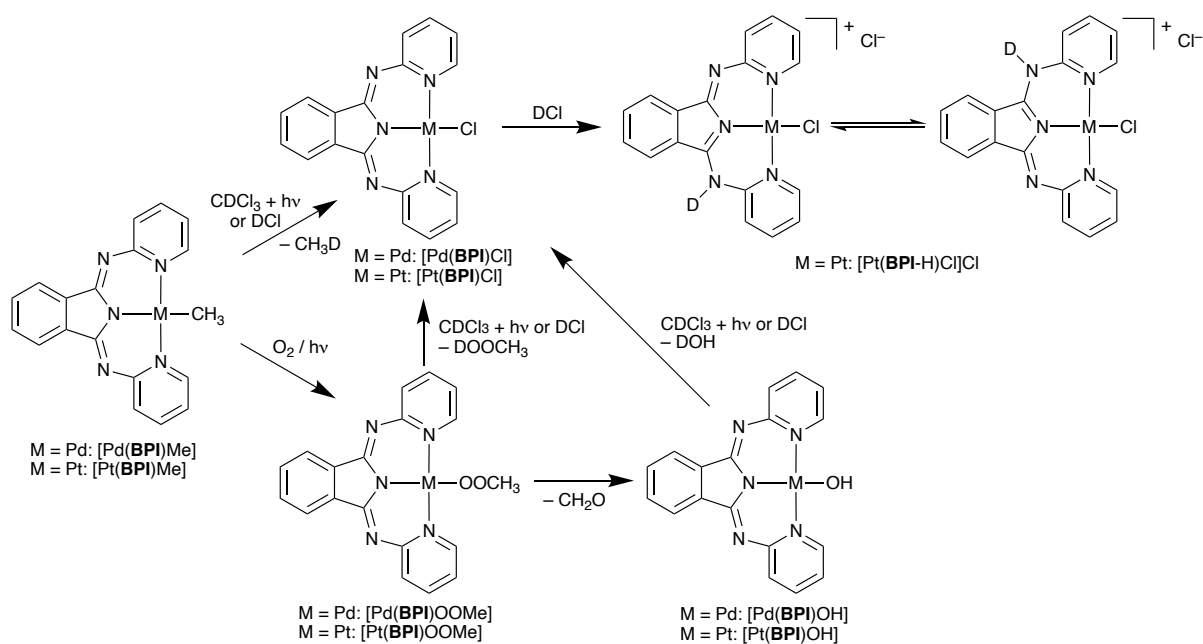
The palladium complex $[\text{Pd}(\text{BPI})\text{Me}]$ is more reactive than the platinum analogue and shows after 4 hours irradiation with UV light in CDCl_3 complete conversion to the chloro complex $[\text{Pd}(\text{BPI})\text{Cl}]$ (see Figure S2). The phenyl complex $[\text{Pt}(\text{BPI})\text{Ph}]$ is remarkably stable

in CDCl₃ upon exposure to UV light for 27 hours at room temperature (See Figure S4). These differences in reactivity for methyl and ethyl versus phenyl complexes are likely related to the M–C bond strengths. The Pt–C bond strength for platinum(II) phenyl complexes is approximately 50 kcal/mol, whereas the BDE for platinum(II)–methyl bonds is significantly smaller, approximately 36 kcal/mol, and approximately 28 kcal/mol for a palladium(II)–methyl bond.⁴⁸⁻⁵¹ Transition metal methyl bonds are generally stronger than ethyl or higher alkyl bonds,⁵²⁻⁵⁴ in line with the different reactivity of [Pt(**BPI**)Et] vs. [Pt(**BPI**)Me] seen here. The formation of methyl chloride and ethyl chloride hints at the involvement of radicals. However, the presence of CH₃D and C₂H₅D suggests protonation of the alkyl complexes could also be involved.

Conversion of platinum(II) and palladium(II) alkyl complexes to chloro complexes upon photolysis in chlorinated solvents is a well-known phenomenon.⁵⁵⁻⁵⁹ These reactions are generally thought to proceed via photoexcitation of the starting complex, followed by homolytic M–C bond cleavage to generate a solvent-caged pair, comprising a methyl radical and an M(I) species. Both radical species can abstract a chlorine radical from the solvent to give methyl chloride and a M(II)–Cl complex, respectively. Oxidative addition of chloroform at Pt(II) centres is also a possibility, but often leads to mixtures of complexes.⁶⁰ The clean formation of the chloro complexes seen here, together with methyl chloride (or ethyl chloride) suggests that homolytic M–C bond cleavage also proceeds with these complexes. There is however, a possible alternative pathway that needs to be considered.

Chloroform decomposes under UV irradiation to generate HCl, together with CCl₂ or phosgene if oxygen is present.⁶¹⁻⁶³ Cleavage of the C–Cl bond requires high energy hard UV-C light with $\lambda < 190$ nm.⁶¹ While chloroform is normally stable towards soft UV-A light of $\lambda = 365$ nm (used here), photo-catalysts such as porphyrins or bis(triazole)phenyl compounds, can lower the energy required for the photo-decomposition of chloroform.⁶³⁻⁶⁴ The formation of chloro complexes [Pt(**BPI**)Cl] and [Pd(**BPI**)Cl], as well as CH₃D under soft UV-A irradiation seen here could be due to a reaction of the alkyl complexes with DCl, generated *in situ* from CDCl₃. The photo-decomposition of CDCl₃ at 365 nm could also be catalysed by the **BPI** complexes used here, although we have not investigated this aspect in any detail. Protonation reactions of platinum(II) alkyl complexes with HCl have been studied extensively and proceed via oxidative addition to form Pt(IV) hydrido alkyl chloro intermediates. These Pt(IV) complexes generally show fast reductive elimination and formation of the Pt(II) chloro complex, although in some cases, the Pt(IV) intermediates can be observed and isolated.⁶⁵

In a separate experiment, $[\text{Pt}(\text{BPI})\text{Me}]$ was reacted with excess DCl (in D_2O) at room temperature. This resulted in quantitative formation of a new complex, which was characterised as the protonated chloro complex $[\text{Pt}(\text{BPI}-\text{D})\text{Cl}]\text{Cl}$ (see Figure S6). Similarly, addition of HCl to the chloro complex $[\text{Pt}(\text{BPI})\text{Cl}]$ in CDCl_3 resulted in protonation of one of the imine groups to give the analogous complex $[\text{Pt}(\text{BPI}-\text{H})\text{Cl}]\text{Cl}$. This complex was characterised by NMR spectroscopy and scXRD analysis (see Supporting Information). A fast proton exchange reaction makes both sides of the ligand appear equivalent (Scheme 1) at room temperature. VT-NMR studies of $[\text{Pt}(\text{BPI}-\text{H})\text{Cl}]\text{Cl}$ in CDCl_3 have shown that the complex becomes asymmetric at lower temperatures, with a coalescence temperature of approximately $T_c = 260 \text{ K}$ in CDCl_3 (see Figure S83). Similar behaviour was seen by Wicholas for a related cadmium complex.⁶⁶ In summary, these studies in the absence of O_2 have shown that both photolysis and protonolysis of the metal carbon bond can take place.



Scheme 1. Reactivity pathways for $[\text{Pt}(\text{BPI})\text{Me}]$ and $[\text{Pd}(\text{BPI})\text{Me}]$ complexes.

Reactivity towards oxygen

The reactivity of the alkyl and aryl BPI complexes towards oxygen (1 atm) was investigated, both with UV light exposure (365 nm) and without. A solution of $[\text{Pt}(\text{BPI})\text{Me}]$ in CDCl_3 , saturated with oxygen (1 atm) was exposed to UV light at room temperature. After 20 minutes, the Pt-Me signal at 1.04 ppm disappeared and a new singlet peak was seen at 3.94 ppm, which corresponds to the methylperoxo complex $[\text{Pt}(\text{BPI})\text{OOCH}_3]$ (see Figure S11 and Scheme 1). Spectroscopic features of this methylperoxo complex are very similar to those seen for the

methylperoxo BPI complexes reported by Goldberg.⁶⁷ The protons at the 6-position of the pyridines are strongly deshielded at 10.44 ppm (c.f. 9.19 ppm for [Pt(**BPI**)Me]), indicating possible hydrogen bonding interactions between these protons and the methylperoxo moiety. Oxygen insertion into the Pt–Me bond at room temperature is also observed when air is used instead of pure oxygen, but the reaction is significantly slower. The oxygen insertion reaction also proceeds in other solvents such as CHCl₃, CD₂Cl₂, CH₂Cl₂, THF-*d*₈ and C₆D₆, albeit with different reaction times (see Figures S12-14, 19 and 20). Reaction times are most affected by light irradiation however. Oxygen insertion proceeds fastest in CDCl₃ or CHCl₃ within approximately 20 minutes upon UV irradiation and 2 days in the dark for full conversion (see Figures S11/S13). In the absence of oxygen, very little (~1%) chloro complex [Pt(**BPI**)Cl] is formed after one day in the dark in CDCl₃. In all chlorinated solvents, regardless whether the reaction with oxygen was performed in the dark or under UV light, the chloro complex [Pt(**BPI**)Cl] is formed in variable amounts together with [Pt(**BPI**)OOMe]. The methylperoxo complex also converts to the chloro complex [Pt(**BPI**)Cl] under these reaction conditions, either due to a photolytic reaction, or due to reaction with DCl generated *in situ* from chloroform (see Scheme 1). DCl reacts with [Pt(**BPI**)Me] to form [Pt(**BPI**)Cl] or with the methylperoxo complex [Pd(**BPI**)OOMe] to give [Pd(**BPI**)Cl], together with CH₃D and CH₃OOD, respectively (Figures S6-S7). A similar conversion of a methylperoxo platinum complex to the corresponding chloro complex was observed by Goldberg in CD₂Cl₂.²³ A clean conversion of [Pt(**BPI**)Me] with oxygen to the methylperoxo complex [Pt(**BPI**)OOMe] can be achieved in THF-*d*₈, when the reaction is kept in the dark for approximately 2 weeks (Figure S14a). Irradiation accelerates the insertion reaction also in THF, but decomposition of the methylperoxo complex takes place before full conversion of the starting methyl complex has been achieved, resulting in complex mixtures of products (Figure S14b). It is thus clear that the oxygen insertion reaction proceeds in various solvents, with or without UV light, but the presence of light strongly accelerates the oxygen insertion reaction.

The palladium methyl complex [Pd(**BPI**)Me] reacts with oxygen (1 bar) in CDCl₃ upon exposure to UV light (365 nm) within 20 minutes to give [Pd(**BPI**)OOMe], together with small amounts of the chloro complex [Pd(**BPI**)Cl] (see Figure S15). The ¹H NMR spectrum features a Pd-OOMe signal at 3.90 ppm and the protons at the 6-position of the pyridine rings at 9.79 ppm. [Pd(**BPI**)OOMe] could be crystallised and the molecular structure was confirmed by X-ray crystallography (see Figure 4). This is the first reported X-ray structure of a palladium(II) methylperoxo complex. A square planar geometry is observed whereby the bond angle of

N(1)-Pd(1)-O(24) is nearly linear with 178.05° and is significantly less distorted than the N(1)-Pd(1)-C(24) angle of $165.3(4)^\circ$ in [Pd(**BPI**)Me]. The O(24)-O(25) bond length of $1.475(4) \text{ \AA}$ is slightly longer than the one in the related BPI platinum complex ($1.419(10) \text{ \AA}$), but comparable to those in other PdOOX complexes ($X = \text{H}, \text{tBu}$),⁶⁸ and PtOOMe complexes,^{23, 25} and shorter than in a related NiOOMe complex ($1.513(2) \text{ \AA}$) (see Figure 1).²⁰ The short distances between O(24) and the protons in 6-position of the pyridines ($2.1\text{-}2.2 \text{ \AA}$) are indicative of a hydrogen bonding interaction, as indicated by the downfield chemical shift of these protons from 8.70 ppm to 9.79 ppm.

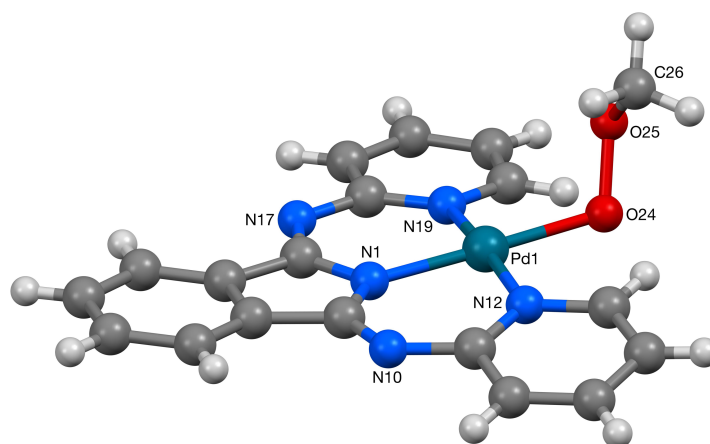


Figure 4. Molecular structure determined by scXRD analysis of [Pd(**BPI**)OOMe].

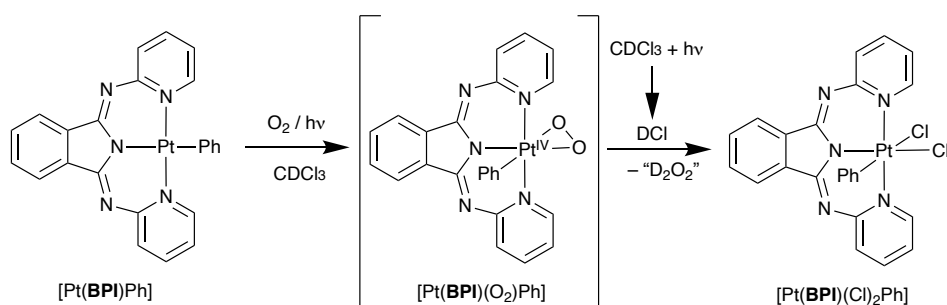
The formation of [Pd(**BPI**)OOMe] is also observed in other solvents, including CHCl_3 , CD_2Cl_2 and $\text{THF-}d_8$, both upon irradiation and in the dark. The reactivity of [Pd(**BPI**)Me] with oxygen is thus very similar to the platinum analogue, whereby complete conversion to [Pd(**BPI**)OOMe] requires approximately 20 minutes of irradiation in CDCl_3 , compared to several weeks in the dark (see Figure S16). The palladium chloro complex [Pd(**BPI**)Cl] is only observed in chlorinated solvents after irradiation with UV light and no chloro complex was detected in the dark after one day. Extensive reactivity studies in various solvents have shown that oxygen insertion for both methyl complexes [Pt(**BPI**)Me] and [Pd(**BPI**)Me] are fastest in CDCl_3 .

The possible involvement of singlet oxygen $^1\text{O}_2$ in the insertion reactions was considered. The addition of 2,2,6,6-tetramethylpiperidine (TEMP) and 1,4-diazabicyclo[2,2,2]-octane (DABCO), which are both known singlet oxygen quenchers, was investigated.⁶⁹⁻⁷¹ The addition of TEMP (8 equivalents) or DABCO (8 equivalents) to a CDCl_3 solution of

[Pt(**BPI**)Me] followed by the addition of oxygen and exposure to UV light (365 nm) did not show any noticeable difference in the oxygen insertion reactivity (see Figures S23 and S24). The methyl peroxy complex [Pt(**BPI**)OOMe] and the chloro complex [Pt(**BPI**)Cl] were observed after irradiation for 20 minutes. We therefore conclude that involvement of singlet oxygen in the oxygen insertion reactions is unlikely.

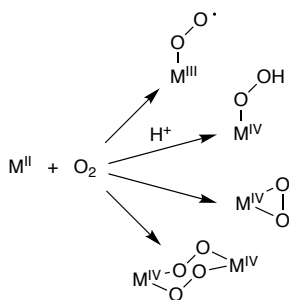
Addition of oxygen to the ethyl complex [Pt(**BPI**)Et] in CDCl₃ at room temperature leads to an immediate colour change from red to orange and clean formation of the ethylperoxy complex [Pt(**BPI**)OOEt]. The characteristic 6-pyridine signal shifts from 9.22 ppm (³J_{PtH} = 52 Hz) for [Pt(**BPI**)Et] to 10.46 ppm (³J_{PtH} = 44 Hz) for [Pt(**BPI**)OOEt], whereas the diagnostic ethylperoxy signals appear at 4.16 and 1.29 ppm. Importantly, the insertion reaction proceeds instantly in the absence of light, compared to 2 days for [Pt(**BPI**)Me]. Fast oxygen insertion occurs also in other solvents such as CD₂Cl₂ and d⁸-THF and again no light is required. The weaker M–C bond for the ethyl complex compared to the methyl complex could be responsible for this difference in reactivity. The different behaviour for methyl versus ethyl bonds in these oxygen insertions is reminiscent of the different rates seen for CO migratory insertion reactions in molybdenum alkyl bonds.⁷²

The platinum phenyl complex [Pt(**BPI**)Ph] reacts with oxygen on exposure to UV light at room temperature, but a different product is obtained in this case. The ¹H NMR spectrum of the starting material features the characteristic 6-pyridine signal at 8.64 ppm (³J_{PtH} = 56 Hz), which disappears after 3 hours irradiation at room temperature to give a new signal downfield at 10.25 ppm with a much smaller coupling constant ³J_{PtH} = 32 Hz (see Figure S21a). The strong downfield shift indicates H-bonding to an O donor ligand. The phenyl signals shift and the ortho-protons move from 7.66 ppm to 6.71 ppm with a Pt-H coupling of ³J_{PtH} = 33 Hz. The phenyl ligand is still directly attached to the Pt centre and the smaller coupling constants indicate the formation of a Pt(IV) complex. We propose that this new complex is the peroxy complex [Pt(**BPI**)(O₂)Ph], as shown in Scheme 2. Analysis by ESI mass spectrometry showed a molecular ion [M]⁺ at *m/z* = 603.1138 (calc. 603.1108 for [Pt(**BPI**)(O₂)PhH]⁺), although several other species are obtained due to protonation under the MS conditions (Figure S21e). The IR spectrum showed a signal for ν(OO) = 773 cm⁻¹ (Figures S21b-d). Side-on peroxy complexes are well known for Pt(II) and ν(OO) stretches are typically around 800-900 cm⁻¹, but there are no reported values for Pt(IV) complexes.⁷³⁻⁷⁵



Scheme 2. Reaction of $[\text{Pt}(\text{BPI})\text{Ph}]$ with O_2 under UV irradiation in CDCl_3 .

The formation of stable side-on peroxo M(III) complexes from the reaction of square planar d^8 metal complexes with oxygen is well known for Group 9.⁷⁶⁻⁷⁹ Noteworthy in particular, are the iridium(III) phenyl complexes with a side-on peroxo ligand, very similar to the Pt(IV) complex seen here, that were reported by Wendt and Milstein.⁸⁰⁻⁸¹ For Pd(II) and Pt(II) complexes, the reaction with oxygen has resulted in a number of products (see Scheme 3).⁸² In addition to side-on peroxo complexes, the formation of a Pd(III) superoxide complex has been observed,²⁹ or in the presence of protic solvents, a hydroperoxo Pt(IV) complex was obtained.⁸³⁻⁸⁴ The formation of a dinuclear Pt(IV) complex with two bridging peroxide ligands is also possible.^{82, 85} The latter has shown an IR stretch $\nu(\text{OO}) = 807 \text{ cm}^{-1}$ for the bridging peroxide moieties.⁸⁵ The possible formation of a bridging bis(peroxide) dinuclear complex $[\text{Pt}(\text{BPI})(\mu\text{-O}_2)\text{Ph}]_2$ was considered, but the lower $\nu(\text{OO}) = 773 \text{ cm}^{-1}$ and the MS data suggest a mononuclear $[\text{Pt}(\text{BPI})(\mu\text{-O}_2)\text{Ph}]$ complex. The peroxo complex $[\text{Pt}(\text{BPI})(\text{O}_2)\text{Ph}]$ showed no reaction towards PPh_3 at room temperature over several days. A similar lack of reactivity was reported for the iridium(III) phenyl peroxide complex.⁸⁰



Scheme 3. Possible reactions seen for Group 10 M^{II} complexes with O_2 .

Further irradiation of the proposed peroxo complex $[\text{Pt}(\mathbf{BPI})(\text{O}_2)\text{Ph}]$ in CDCl_3 results in the formation of a new Pt(IV) complex, with ^1H NMR signals for the 6-pyridine protons at 9.95 ppm ($^3J_{\text{PtH}} = 36$ Hz) and the ortho-phenyl protons at 6.32 ppm ($^3J_{\text{PtH}} = 32$ Hz). This complex was crystallised from a chloroform solution and X-ray analysis (see Figure 5) confirmed the structure as the Pt(IV) complex $[\text{Pt}(\mathbf{BPI})(\text{Cl})_2\text{Ph}]$. This complex $[\text{Pt}(\mathbf{BPI})(\text{Cl})_2\text{Ph}]$ is a rare example of a Pt(IV) complex containing the BPI ligand. The formation presumably occurs via protonation with DCl and in situ generation of D_2O_2 , as seen previously for other metal peroxide complexes,⁷⁵ but this was not further investigated. The proposed side-on peroxo complex $[\text{Pt}(\mathbf{BPI})(\text{O}_2)\text{Ph}]$ would be structurally similar to this dichloro complex.

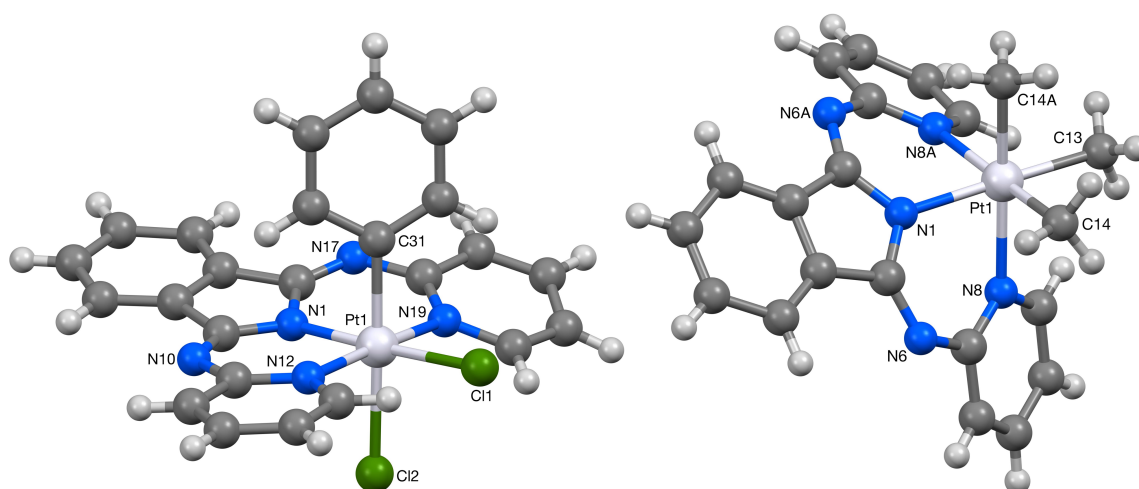
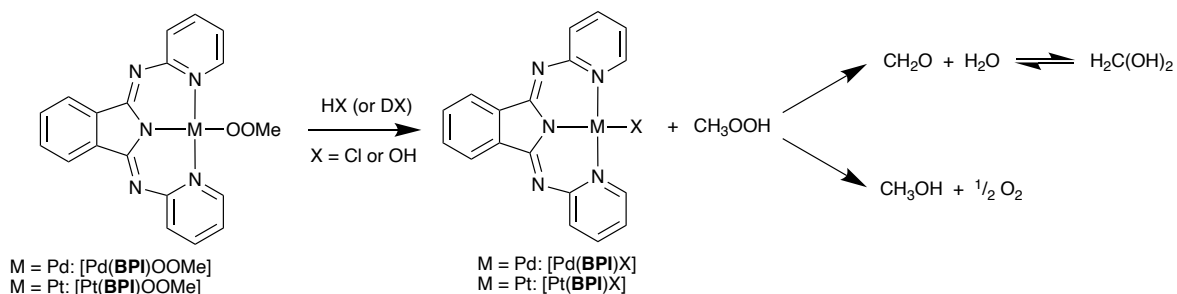


Figure 5. Molecular structures determined by scXRD analysis for Pt(IV) complexes $[\text{Pt}(\mathbf{BPI})(\text{Cl})_2\text{Ph}]$ and $[\text{Pt}(\mathbf{BPI})(\text{CD}_3)_3]$.

Reactivity of the methylperoxo complexes

While the methylperoxo complexes $[\text{Pt}(\mathbf{BPI})\text{OOMe}]$ and $[\text{Pd}(\mathbf{BPI})\text{OOMe}]$ can be isolated and characterised, they do undergo further reaction upon UV irradiation in CDCl_3 solution. In the case of platinum, a new complex with a signal at 10.66 ppm ($^3J_{\text{Pt-H}} = 40$ Hz) together with a sharp singlet at 9.74 ppm is observed, in addition to the chloro complex $[\text{Pt}(\mathbf{BPI})\text{Cl}]$. These signals are assigned to the hydroxo complex $[\text{Pt}(\mathbf{BPI})\text{OH}]$ and formaldehyde, respectively (see Figure S9/S10 and Scheme 4). Methyl hydroperoxide and other alkyl hydroperoxides are known to decompose to the corresponding aldehyde and water, especially under basic conditions.⁸⁶⁻⁸⁷ During the course of approximately 20 minutes at room temperature, the signals for $[\text{Pt}(\mathbf{BPI})\text{OOMe}]$ and $[\text{Pt}(\mathbf{BPI})\text{OH}]$ disappear in favour of the chloro complex $[\text{Pt}(\mathbf{BPI})\text{Cl}]$ at 10.31 ppm, likely due to reaction with DCl generated from CDCl_3 . The hydroxo

complex [Pt(**BPI**)OH] was prepared independently by reacting the chloro complex with excess KOH in THF under reflux and the NMR spectrum confirmed the assignments (see Supporting Information). Similar hydroxo complexes of platinum(II) with BPI ligands were recently reported by Goldberg and their spectroscopic features correspond to those seen here.³⁸



Scheme 4. Reactivity of methylperoxo complexes.

The formaldehyde signal at 9.74 ppm decreases over time and a new signal is formed at 4.75 ppm for methane diol $\text{H}_2\text{C(OH)}_2$ from the reaction with water (or HDO).⁸⁸ Additional organic products observed are methyl hydroperoxide and methanol at 3.84 ppm and 3.44 ppm, respectively.²⁴ Methyl deuterioperoxide (MeOOD), likely formed from [Pt(**BPI**)OOMe] upon protonation with DCl , is unstable and decomposes, depending on conditions, either to methanol and oxygen (analogous to the decomposition of H_2O_2 to water and oxygen) or to formaldehyde and water under basic conditions (see Scheme 2).⁸⁸⁻⁸⁹ Further products observed are methyl chloroformate and dimethyl carbonate, at 3.96 ppm and 3.79 ppm, respectively. These products originate from the reaction of methanol with phosgene, the latter being generated from chloroform under UV irradiation in the presence of oxygen.⁶¹⁻⁶³ In a separate experiment, a solution of methanol in CDCl_3 was saturated with oxygen and exposed to UV light irradiation. After 16 hours, nearly complete conversion of methanol to methyl chloroformate (3.96 ppm), formic acid (8.01 ppm) and methyl formate (8.07 and 3.76 ppm) was observed (see Figure S8). Oxidative degradation of chloroform under UV irradiation is well documented and involves several reactive intermediates such as phosgene and formyl chloride that could lead to these products.⁹⁰ The palladium methylperoxo complex [Pd(**BPI**)OOMe] undergoes a similar decomposition pathway as [Pt(**BPI**)OOMe] and a similar product spectrum consisting of formaldehyde, methanol, methyl chloroformate and dimethyl carbonate is observed (see Figure S15).

The fate of the ethylperoxo complex [Pt(**BPI**)OOEt] upon UV irradiation was monitored in several solvents and appears to be very similar to the methylperoxo complex. In CDCl_3 , the

characteristic downfield signal for the 6-pyridine protons at 10.46 ppm ($^3J_{\text{PtH}} = 44$ Hz) disappears during the course of 15 minutes UV exposure and the formation of $[\text{Pt}(\mathbf{BPI})\text{Cl}]$ is observed together with new signals at 9.8 ppm corresponding to acetaldehyde and at 3.72 and 1.25 ppm for ethanol (see Figure S17).

Deuterium labelling studies

In order to trace the methyl ligand in $[\text{Pt}(\mathbf{BPI})\text{Me}]$ and the fate of the methyl protons after reaction with oxygen, we prepared the deuterated complex $[\text{Pt}(\mathbf{BPI})\text{CD}_3]$. During the synthesis of $[\text{Pd}(\mathbf{BPI})\text{CD}_3]$, the formation of a minor by-product was noticed, which was isolated and characterised as the platinum(IV) complex $[\text{Pt}(\mathbf{BPI})(\text{CD}_3)_3]$ by X-ray crystallography (see Figure 5 and Supporting information). The formation of this Pt(IV) complex is likely due to some decomposition of the starting complex $[\text{PtI}(\text{CD}_3)(\text{SMe}_2)_2]$. Formation of CD_3I together with methyl exchange reactions can result in the known Pt(IV) complexes $[\text{PtI}(\text{CD}_3)_3(\text{SMe}_2)_2]$ or $[\text{Pt}_2\text{I}_2(\text{CD}_3)_6(\text{SMe}_2)_2]$,⁹¹ and their reaction with $\mathbf{BPI}\text{-K}$ would lead to $[\text{Pt}(\mathbf{BPI})(\text{CD}_3)_3]$. The non-deuterated complex $[\text{Pt}(\mathbf{BPI})(\text{CH}_3)_3]$ was prepared independently from $\mathbf{BPI}\text{-K}$ and $[\text{Pt}(\text{CH}_3)_3(\text{OTf})]_4$ and was fully characterised (see Supporting Information). A structurally interesting feature of this complex is that the \mathbf{BPI} ligand adopts a rather strained and unusual facial coordination mode, which hitherto has not been reported for this ligand. This is most likely due to the reluctance of methyl ligands with their strong trans influence to coordinate trans to each other. $[\text{Pt}(\mathbf{BPI})(\text{CH}_3)_3]$ was found to be stable in CDCl_3 and $1,2\text{-C}_2\text{D}_2\text{Cl}_4$ over the temperature range from 213 K to 373 K (see Figures S80/S81) and did not react with oxygen upon exposure to UV light for 4 hours. For comparison, other Pt(IV) complexes have shown reactivity towards light and oxygen, but no oxygen insertion into Pt-CH₃ bonds. For example, $[\text{Pt}(\text{bipy})(\text{CH}_3)_4]$ reacts in chlorinated solvent under UV irradiation to give $[\text{PtCl}(\text{bipy})(\text{CH}_3)_3]$.⁹² A five-coordinate Pt(IV) trimethyl complex $[\text{Pt}(\mathbf{L})(\text{CH}_3)_3]$, featuring a bidentate diketiminate ligand \mathbf{L} , was reported to react with oxygen,⁹³ but in this case the diketiminate ligand reacts with oxygen, rather than oxygen insertion into the metal methyl bond. Furthermore, the six-coordinate Pt(IV) complexes $[\text{PtTp}^*\text{HR}_2]$, where R = Me or Ph and Tp^* is the anionic facially-coordinating tris(pyrazolyl)borate ligand, was found to react with O_2 to result in insertion into the Pt-H bond to give a hydroperoxide complex $[\text{PtTp}^*(\text{OOH})\text{R}_2]$.⁹⁴

A CHCl_3 solution of $[\text{Pt}(\mathbf{BPI})\text{CD}_3]$ was saturated with oxygen and exposed to UV light. After irradiation for 8 minutes, the ^2H NMR signal of the methyl peroxy species

[Pt(**BPI**)(OOCd₃)] was observed at 3.87 ppm as shown in Figure 6. This complex undergoes further reaction over time, leading initially to CD₃OH and CD₃OOH at 3.4 ppm and 3.8 ppm, respectively. Over the course of an hour under UV irradiation, methanol reacts with phosgene from CHCl₃ decomposition to give methyl chloroformate and dimethyl carbonate. The amount of water (D₂O/HDO) at 1.5 ppm increases over time, which supports the notion that water is being generated during the decomposition of CD₃OOH to formaldehyde. Formaldehyde is however not seen in the ²H NMR spectra (at 9.7 ppm) but multiple signals are observed at 4.6-5 ppm after exposure to UV light, which can be assigned to methanediol ($\delta(\text{CD}_2) = 4.94$ ppm) from the reaction of formaldehyde with water,⁸⁸ as well as methoxymethanol ($\delta(\text{CD}_2) = 4.67$ ppm and $\delta(\text{CD}_3) = 3.37$ ppm)⁹⁵ which originates from the reaction of formaldehyde with methanol. Overall, we can conclude that the original methyl ligand in [Pt(**BPI**)(OOCd₃)] eventually ends up either as methanol (or a methanol derivative), or as formaldehyde (or formaldehyde derivative) and the ratio between these products will depend on the reaction conditions.

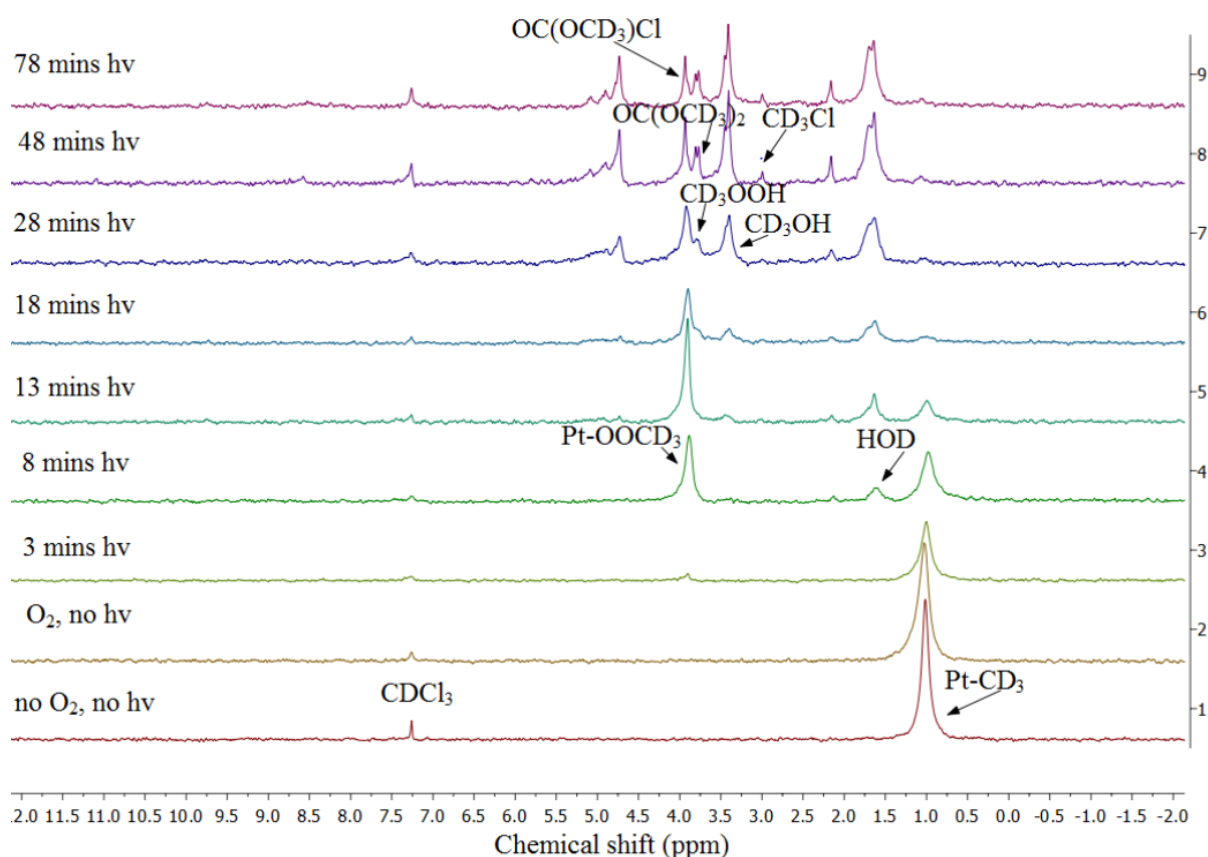


Figure 6. ²H NMR spectra for the reaction of [Pt(**BPI**)CD₃] with oxygen in CHCl₃ solution at 298 K upon exposure to UV light (365 nm).

An equimolar mixture of [Pt(**BPI**)CD₃] and [Pd(**BPI**)CH₃] was mixed in CDCl₃ and reacted with O₂. The reaction mixture was exposed to UV light (365 nm) and the reaction was monitored by ¹H NMR spectroscopy (Figure S25). Prior to UV irradiation and exposure to oxygen, only the Pd-CH₃ proton signal is observed. After the reaction mixture was saturated with oxygen and exposed to UV light for 3 minutes, the Pd-OOMe signal and the Pt-OOMe signal appear at 3.89 ppm and 3.94 ppm, respectively. These methylperoxo complexes decompose over time to methyl hydroperoxide and the corresponding chloro complexes, as seen previously above. The reaction was repeated in CHCl₃ and monitored by ²H NMR spectroscopy (Figure S26). Before exposure to UV light, only one singlet was observed at 1.01 ppm, assigned to [Pt(**BPI**)CD₃]. The reaction mixture was exposed to UV light for 15 minutes in the absence of oxygen. Interestingly, no methyl exchange between [Pt(**BPI**)CD₃] and [Pd(**BPI**)CH₃] was observed within this time. The reaction mixture was then saturated with oxygen and exposed to UV light. After 11 minutes of UV irradiation, the Pt-CD₃ signal disappeared and a broad signal appeared at 3.79 – 4.01 ppm with a small splitting. The broad signal consists of the Pt-OOCD₃ signal at 3.90 ppm and the Pd-OOCD₃ signal at 3.87 ppm. In a separate experiment, [Pt(**BPI**)OOCD₃] and [Pd(**BPI**)OOCH₃] were prepared independently in CDCl₃, then mixed and exposed to UV light for 10 minutes, revealing both [Pt(**BPI**)OOCH₃] and [Pd(**BPI**)OOCH₃] in the ¹H NMR spectrum, along with the formation of the chloro complexes. These experiments confirm that exchange occurs between the methylperoxo ligands, but not between the methyl ligands. The possibility that exchange occurs *during* the oxygen insertion reaction between methylperoxo and methyl ligands cannot be excluded at this stage. Upon prolonged exposure to UV light, all methylperoxo complexes decompose to generate the chloro complexes as well as methanol and the usual products dimethylcarbonate (3.77 ppm), methyl chloroformate (3.91 ppm) and methanediol (4.73 ppm). A small amount of methyl chloride (2.98 ppm) was also observed. To conclude, methyl exchange between [Pt(**BPI**)CD₃] and [Pd(**BPI**)CH₃] did not occur in the absence of oxygen upon exposure to UV light for 15 minutes. Once the reaction mixture was saturated with oxygen, a mixture of [Pt(**BPI**)OOCD₃], [Pt(**BPI**)OOCH₃], [Pd(**BPI**)OOCD₃] and [Pd(**BPI**)OOCH₃] was formed upon UV irradiation due to the exchange between methylperoxo ligands. It is likely that the Pt-O bond is weaker than the Pt-C bond,⁹⁶ which allows ligand exchange to occur between the methylperoxo complexes but not between the methyl complexes.

Computational studies

Various mechanisms have been proposed for the oxygen insertion reaction into metal-carbon,^{11, 24, 97-98} and metal-hydride bonds.⁹⁹⁻¹⁰³ A radical chain mechanism is generally proposed for main group metal alkyls such as magnesium,¹⁰⁴ boron and aluminium alkyl compounds, and also for certain transition metal alkyl complexes, in particular where oxidation of the metal is not possible, for example zinc alkyls.²¹ For $[L_nM]^{n+}$ complexes where an $(n+2)$ oxidation state is easily accessible, the formation of side-on peroxide complexes $[L_nM(\kappa^2-O_2)]^{(n+2)+}$ is frequently observed, notably for Rh(III) and Ir(III).⁷⁶⁻⁷⁹

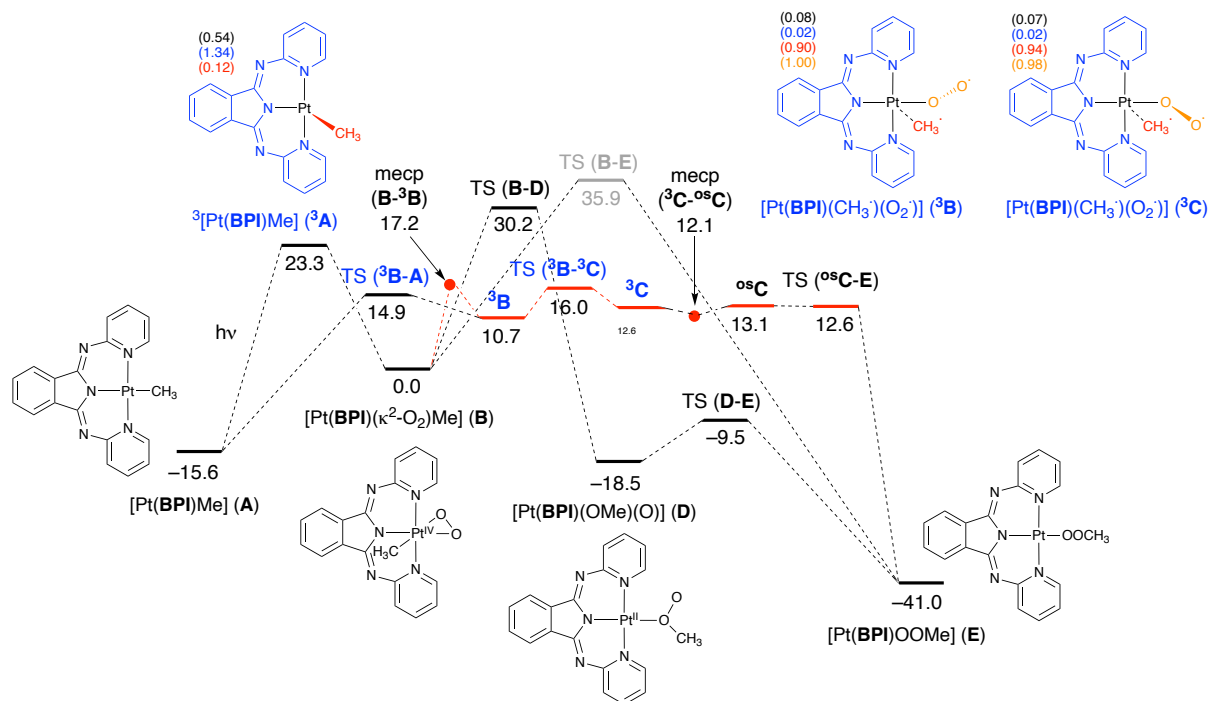
Goldberg and co-workers have previously reported that for palladium(II) and platinum(II) methyl complexes with BPI-type ligands, oxygen insertion proceeds via a radical chain mechanism based on kinetic studies.⁶⁷ In order to obtain reproducible kinetic results, AIBN was used as a radical initiator in their experiments. The oxygen insertion reactions seen here do proceed in the absence of light, albeit very slowly over the course of several days or weeks depending on the reaction conditions. These insertion reactions in the dark may well proceed via a slow radical chain reaction, but how do we account for the tremendous rate acceleration in the presence of light? The acceleration by light of the reaction with oxygen in these palladium and platinum alkyl complexes suggests the involvement of excited state intermediates. Is it possible that radical chain reactions proceed within the coordination sphere of the metal centre? The coordination behaviour of triplet state intermediates and their chemical reactivity is largely unknown, not least because these reactions are difficult to study experimentally. Computational studies using density functional theory (DFT) can be used to scan potential energy surfaces and determine the energy of the minimum energy crossing points (mecp) between different spin states.¹⁰⁵ Previous DFT studies on oxygen insertion reactions of terpyridine platinum(II) methyl complexes have shown that Pt(IV) side-on peroxide complexes $[(\text{terpy})M(\kappa^2-O_2)]^+$ as reaction intermediates are a distinct possibility. Subsequent reductive coupling results in C–O bond formation to give the Pt(II) methyl peroxo complexes.¹⁰⁶ We have carried out computational studies on the BPI complexes studied here to establish whether a similar pathway also applies for the oxygen insertion reactions seen here.

Computational studies have been carried out using the same method that we used in our previous calculations on oxygen insertions with terpyridine Pt(II) complexes, except that a different solvent (CHCl_3) was used here.¹⁰⁶ The method, fully outlined in the Supporting Information, involves the use of the M06 functional, and all results reported below correspond

to Gibbs free energies. The validity of the functional and the basis set were benchmarked in our previous work on a similar system.¹⁰⁶ All computational results are collected in the ioChem-BD repository.¹⁰⁷

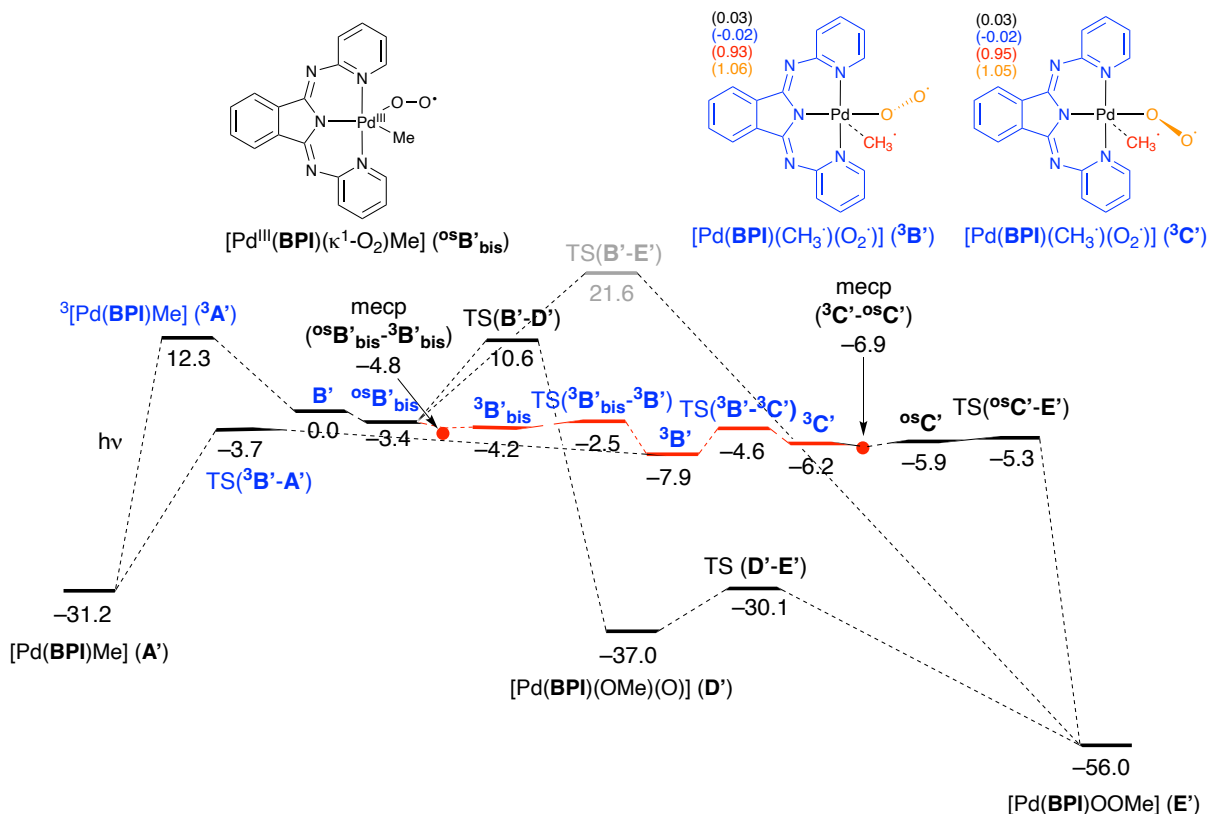
Good agreement was generally observed between the calculated bond distances and angles and the experimental values determined by XRD analysis for the complexes [Pt(**BPI**)Me], [Pd(**BPI**)Me] and [Pd(**BPI**)OOMe] (see Table S2). TD-DFT studies on the oxygen insertion reaction with [Pt(**BPI**)Me] have shown that the formation of the Pt(IV) peroxide intermediate is indeed energetically feasible. Initial excitation of the square planar starting complex [Pt(**BPI**)Me] (**A**) involves an electron transfer from a metal d orbital to a ligand π^* orbital (MLCT) (see Scheme 5). After intersystem crossing this leads to a metastable triplet complex 3 [Pt(**BPI**)Me] (3 **A**), where the methyl ligand is severely bent out of the coordination plane (N–Pt–C angle: 148.9°, cf. 167.8° in complex **A**) and with considerable spin density on the BPI ligand (1.34) and the metal (0.54), with some residual spin density residing on the methyl ligand. The Pt–C bond distances are very similar, with 2.06 Å for 3 **A** compare to 2.07 Å in **A**. This triplet intermediate 3 **A** may dimerise, as we have previously suggested for the terpyridine complexes,²⁶ but according to computational studies, this did not affect the subsequent reactivity with oxygen.¹⁰⁶ We have therefore not considered the formation of excited state dimeric intermediates for these BPI complexes. The high energy photo-initiated triplet complex 3 **A** at 38.9 kcal/mol rapidly reacts with triplet oxygen to give the side-on M(IV) peroxide complex [Pt(**BPI**)(O₂)Me] (**B**) in the singlet spin state, which is 23.3 kcal/mol lower in energy and 15.6 kcal/mol above the starting complex **A** (all subsequent energies are relative to complex **B**). The reaction with oxygen has no enthalpic barrier, but a small entropic barrier can be estimated of approximately 8 kcal/mol, similar to the value determined previously for the terpyridine complex.¹⁰⁶ From this intermediate [Pt(**BPI**)(O₂)Me] (**B**), reductive coupling with C–O bond formation is in principle possible on the singlet surface, either via a stepwise process involving intermediate **D**, or via a direct conversion to **E**. In both cases however, the transition states **TS(B-D)** and **TS(B-E)** are rather high at 30.2 and 35.9 kcal/mol, respectively (see Figure S28 for more information on transition states). Further computational studies on intermediate **B** have shown that for this BPI Pt(IV) complex, an alternative energetically much lower pathway exists via thermally induced spin-crossing from **B** to a triplet state 3 **B** at 10.7 kcal/mol, accessible via **MECP(B- 3 B)** at 17.2 kcal/mol. This 3 **B** intermediate has a weakened Pt–C bond and spin densities are located predominantly on the methyl ligand (0.90) and the end-on O₂ (1.00) ligand, best described as 3 [Pt(**BPI**)(CH₃')(O₂')]. Single electron metal ligand

bonds are less common in the ground state,¹⁰⁸⁻¹⁰⁹ but are commonplace in excited-state complexes due to charge transfer. An alternative isomeric complex ${}^3\mathbf{B}_{\text{bis}}$, where the spin density is located on the end-on O_2 ligand (1.01) and the BPI ligand (1.02), rather than on the methyl ligand, *i.e.* ${}^3[\text{Pt}(\mathbf{BPI})(\text{CH}_3)(\text{O}_2)]$, was discarded because of its higher free energy (18.8 kcal/mol). The triplet intermediate ${}^3\mathbf{B}$ can rearrange via rotation around the Pt–O bond (($\text{TS}({}^3\mathbf{B}-{}^3\mathbf{C})$) at 16.0 kcal/mol), to give initially ${}^3\mathbf{C}$ at 12.6 kcal/mol with spin densities on methyl (0.94) and the end-on O_2 (0.98) ligands. The triplet structure ${}^3\mathbf{C}$, with clear spacial separation between the two unpaired electrons, is very close in energy to the corresponding open-shell singlet complex ${}^{\text{os}}\mathbf{C}$ at 13.1 kcal/mol, which can be reached via a MECP at 12.1 kcal/mol. This ${}^{\text{os}}\mathbf{C}$ species, with spin densities on methyl (0.93) and the end-on O_2 ligand (–0.98), is best described as an open shell Pt(II) superoxide complex with a coordinated methyl radical. Final conversion to the methylperoxo complex \mathbf{E} from ${}^{\text{os}}\mathbf{C}$ was found to be barrierless. Instead of going forward, the triplet intermediate ${}^3\mathbf{B}$ can also eliminate O_2 and revert to the starting material \mathbf{A} . This process has a barrier via transition state $\text{TS}({}^3\mathbf{B}-\mathbf{A})$ of 14.9 kcal/mol, which is similar in magnitude to $\text{TS}({}^3\mathbf{B}-{}^3\mathbf{C})$ of 16.0 kcal/mol, suggesting that there is likely to be a competition between oxygen coordination/insertion (\mathbf{A} via ${}^3\mathbf{B}$ to \mathbf{E}) and oxygen coordination/de-coordination (\mathbf{A} via ${}^3\mathbf{B}$ back to \mathbf{A}).



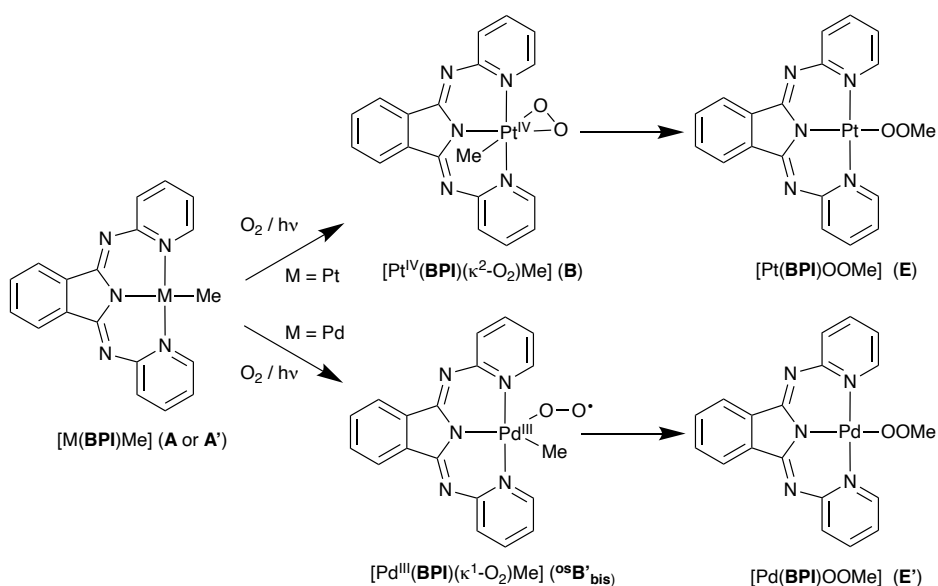
Scheme 5. Reaction profile with Gibbs free energies (kcal/mol) for the reaction of $[\text{Pt}(\mathbf{BPI})\text{Me}]$ with O_2 . Numbers in parentheses are spin densities.

For palladium, the excited state complex $^3[\text{Pd}(\text{BPI})\text{Me}]$ ($^3\text{A}'$), which is 43.5 kcal/mol above the ground state complex $[\text{Pd}(\text{BPI})\text{Me}]$ (A'), is readily quenched by O_2 to give in this case an open shell Pd(III) superoxide complex $^{\text{os}}\text{B}'_{\text{bis}}$ as the most stable singlet state intermediate (see Scheme 6 and Figure S30). This key Pd(III) intermediate has spin densities mostly on the metal (-0.50) and the O_2^- ligand (1.09) and is slightly more stable by 3.4 kcal/mol compared to the Pd(IV) peroxo complex $[\text{Pd}(\text{BPI})(\text{O}_2)\text{Me}]$ (B'), in line with the general lower stability of Pd(IV) versus Pt(IV) complexes.¹¹⁰⁻¹¹¹ Upon excitation, the Pd(III) superoxide complex $^{\text{os}}\text{B}'_{\text{bis}}$ undergoes several transformations via a series of triplet intermediates $^3\text{B}'_{\text{bis}}$, $^3\text{B}'$ and $^3\text{C}'$, all with similar energies, to convert eventually to the open shell Pd(II) superoxide complex ($^{\text{os}}\text{C}'$) with a coordinated methyl radical, with spin densities on methyl (0.94) and superoxide ligand (-1.06). The final conversion of the singlet intermediate $^{\text{os}}\text{C}'$ to the methylperoxo product $[\text{Pd}(\text{BPI})(\text{OOMe})]$ (E') is essentially barrierless. Alternative pathways from the stable Pd(III) intermediate $^{\text{os}}\text{B}'_{\text{bis}}$, either via methyl migration to give intermediate D' , or directly to the product E' were found to be energetically non-competitive. As in the case of Pt, the triplet intermediate $^3\text{B}'$ at -7.9 kcal/mol can eliminate O_2 and revert to the starting complex A' , with a very modest barrier $\text{TS}(^3\text{B}'-\text{A}')$ at -3.7 kcal/mol and there is likely to be a competition between forward and reverse reactions for this intermediate. Alternative pathways via $\text{TS}(\text{B}'-\text{D}')$ and $\text{TS}(\text{B}'-\text{E}')$ were also considered but were found to be non-competitive (see Figure S31 for all Pd transition states).



Scheme 6. Reaction profile with Gibbs free energies (kcal/mol) for the reaction of $[\text{Pd}(\text{BPI})\text{Me}]$ with O_2 . Numbers in parentheses are spin densities.

Overall, we can conclude from these calculations that in the case of $[\text{Pt}(\text{BPI})\text{Me}]$, the oxygen insertion process proceeds via an oxidative addition to form a Pt(IV) side-on peroxide intermediate $[\text{Pt}(\text{BPI})(\kappa^2\text{-O}_2)\text{Me}]$, whereas in the case of $[\text{Pd}(\text{BPI})\text{Me}]$, the O_2 insertion proceeds via a Pd(III) end-on superoxide complex $[\text{Pd}(\text{BPI})(\kappa^1\text{-O}_2)(\text{Me})]$, as shown in Scheme 7 below. A similar methylperoxide complex $[\text{M}(\text{BPI})\text{OOMe}]$ is generated from these different intermediates.



Scheme 7. Overall reactivity of $[\text{M}(\text{BPI})\text{Me}]$ complexes with O_2 .

Conclusions

The overall picture that has emerged from our combined experimental and theoretical studies on the reactivity of BPI platinum and palladium alkyl and aryl complexes $[\text{M}(\text{BPI})\text{R}]$ in the presence of light and oxygen has shown some important insights. In CDCl_3 , in the absence of oxygen, UV irradiation of alkyl complexes results in the formation of chloro complexes $[\text{M}(\text{BPI})\text{Cl}]$, together with RD. This reactivity is attributed to an excitation of the alkyl complexes, which weakens the metal carbon bond and can lead to $\text{R}\cdot$ radicals which can react with the solvent. In addition, the *in situ* formation of DCl upon irradiation of chloroform does also take place, which can react with the starting complexes via a protonolysis reaction. The platinum complex where $\text{R} = \text{Ph}$ is stable under these conditions due to a stronger metal carbon bond.

In the presence of oxygen, alkylperoxide complexes $[\text{M}(\text{BPI})\text{OOR}]$ are formed in various solvents, which in chlorinated solvents react with DCl to form $[\text{M}(\text{BPI})\text{Cl}]$ and various oxidation products derived from ROOD. In the case of $\text{R} = \text{phenyl}$, the formation of a Pt(IV) side-on peroxide complex is proposed $[\text{Pt}(\text{BPI})(\kappa^2\text{-O}_2)\text{Ph}]$, which reacts with DCl to form $[\text{Pt}(\text{BPI})(\text{Cl})_2\text{Ph}]$. The fate of the alkylperoxo complexes was investigated using the labelled complex $[\text{Pt}(\text{BPI})\text{CD}_3]$. The original methyl ligand in $[\text{Pt}(\text{BPI})(\text{OOCd}_3)]$ eventually ends up either as methanol (or a methanol derivative), or as formaldehyde (or a formaldehyde derivative) and the ratio between these products will depend on the reaction conditions.

The reactivity of the palladium and platinum BPI complexes with oxygen and light seen experimentally is reproduced in all cases by DFT calculations. The reaction of both complexes towards light involves the absorption of a photon by the starting BPI complex $[M(\mathbf{BPI})R]$, which evolves to a triplet intermediate that is able to react with oxygen. The two metals differ on the rather complicated multistep mechanisms in that for platinum, the reaction proceeds via a Pt(IV) side-on peroxide intermediate, whereas for palladium an open shell Pd(III) end-on superoxide intermediate is involved. Both reactions eventually result in an oxygen insertion reaction to give the metal alkylperoxide complexes $[M(\mathbf{BPI})OOR]$, but always in competition with a non-productive reversion to separate reactants. The complexity itself of the mechanism confirms the need of a subtle combination of electronic and steric factors in ligands and metal for this reactivity to take place.

The numerous intermediates and transition states in various spin states encountered here by TD-DFT analysis, several of which contain alkyl, superoxyl or peroxy ligands coordinated by one-electron bonds, suggests that these oxygen insertions proceed via radical reactions that take place within the coordination sphere of the metal. The alkylperoxo complexes generated under the influence of light may also generate alkylperoxo radicals upon irradiation which could react with the starting alkyl complex to induce further O_2 insertion reactions, resulting in an overall metal-mediated radical chain reaction. We are continuing our efforts to unravel the finer details of these intriguing insertion reactions.

ASSOCIATED CONTENT

Supporting Information.

Materials and methods, synthetic procedures, NMR and UV-vis spectra, DFT calculations, XRD analysis. All computational results are collected in the ioChem-BD repository,¹⁰⁷ accessible via:

<https://iochem-bd.iciq.es/browse/review-collection/100/29409/f62a2f649af633d06bb2dd02>.

AUTHOR INFORMATION

Corresponding Author

George J.P. Britovsek – *Department of Chemistry, Imperial College London, Molecular Sciences Research Hub, White City Campus, 82 Wood Lane, London W12 0BZ, United Kingdom.* Orcid.org: 0000-0001-9321-4814/ Email: g.britovsek@imperial.ac.uk

Authors

Sarah K.Y. Ho – *Department of Chemistry, Imperial College London, Molecular Sciences Research Hub, White City Campus, 82 Wood Lane, London W12 0BZ, United Kingdom.* Email: kwok.ho12@imperial.ac.uk

Francis Y.T. Lam – *Department of Chemistry, Imperial College London, Molecular Sciences Research Hub, White City Campus, 82 Wood Lane, London W12 0BZ, United Kingdom.* Email: francislam@berkeley.edu

Andrew J.P. White – *Department of Chemistry, Imperial College London, Molecular Sciences Research Hub, White City Campus, 82 Wood Lane, London W12 0BZ, United Kingdom.* Orcid: 0000-0001-6175-1607. Email: a.white@imperial.ac.uk

Adiran de Aguirre – *Institute of Chemical Research of Catalonia, The Barcelona Institute for Science and Technology, Avgda. Països Catalans, 16, Tarragona 43007, Catalonia, Spain.* Orcid: 0000-0001-7991-6406. Email: Adiran-Josu.DeAguirreFondevila@unige.ch

Feliu Maseras – *Institute of Chemical Research of Catalonia, The Barcelona Institute for Science and Technology, Avgda. Països Catalans, 16, Tarragona 43007, Catalonia, Spain.* Orcid: 0000-0001-8806-2019. Email: fmaseras@icmq.es

Notes

The authors declare no competing financial interest.

ACKNOWLEDGMENTS

S.K.S. is grateful for funding from the Stevenson Fund at Imperial College London. A. de A. thanks MINECO for a FPI Fellowship (BES-2015-073012).

REFERENCES

1. Malakoff, D., The gas surge. *Science* **2014**, *344*, 1464-1467.
2. Zichittella, G.; Pérez-Ramírez, J., Status and prospects of the decentralised valorisation of natural gas into energy and energy carriers. *Chem. Soc. Rev.* **2021**, *50*, 2984-3012.
3. Chen, S.; Chang, X.; Sun, G.; Zhang, T.; Xu, Y.; Wang, Y.; Pei, C.; Gong, J., Propane dehydrogenation: catalyst development, new chemistry, and emerging technologies. *Chem. Soc. Rev.* **2021**, *50*, 3315-3354.
4. Alper, J., The Changing Landscape of Hydrocarbon Feedstocks for Chemical Production: Implications for Catalysis: Proceedings of a Workshop. The National Academies Press: Washington, DC, 2016. DOI: 10.17226/23555.
5. Hashiguchi, B. G.; Bischof, S. M.; Konnick, M. M.; Periana, R. A., Designing Catalysts for Functionalization of Unactivated C–H Bonds Based on the CH Activation Reaction. *Acc. Chem. Res.* **2012**, *45*, 885-898.
6. Crabtree, R. H., Alkane C-H activation and functionalisation. *J. Chem. Soc., Dalton Trans.* **2001**, 2437-2450.
7. Stahl, S. S.; Labinger, J. A.; Bercaw, J. E., Homogeneous Oxidation of Alkanes by electrophilic late transition metals. *Angew. Chem. Int. Ed.* **1998**, *37*, 2180-2192.
8. Fekl, U.; Goldberg, K. I., Homogeneous hydrocarbon C-H bond activation and functionalization with platinum. *Adv. Inorg. Chem.* **2003**, *54*, 259-320.
9. Lersch, M.; Tilset, M., Mechanistic aspects of C-H activation by Pt complexes. *Chem. Rev.* **2005**, *105*, 2471-2526.
10. Vedernikov, A. N., Direct functionalization of M-C (M = Pt(II), Pd(II)) bonds using environmentally benign oxidants, O₂ and H₂O₂. *Acc. Chem. Res.* **2012**, *45*, 803-813.
11. Boisvert, L.; Goldberg, K. I., Reactions of late transition metal complexes with molecular oxygen. *Acc. Chem. Res.* **2012**, *45*, 899-910.
12. Pellarin, K. R.; McCready, M. S.; Puddephatt, R. J., Oxidation of Dimethylplatinum(II) Complexes with a Dioxirane: The Viability of Oxoplatinum(IV) Intermediates. *Organometallics* **2012**, *31*, 6388-6394.
13. Rostovtsev, V. V.; Henling, L. M.; Labinger, J. A.; Bercaw, J. E., Structural and mechanistic investigations of the oxidation of dimethylplatinum(II) complexes by dioxygen. *Inorg. Chem.* **2002**, *41*, 3608-3619.
14. Hess, A.; Hörz, M. R.; Liable-Sands, L. M.; Lindner, D. C.; Rheingold, A. L.; Theopold, K. H., Insertion of O₂ into a Chromium-Phenyl Bond: Mechanism of Formation of the Paramagnetic d² Oxo Complex [TptBu₂MeCr^{IV}(O)OPh]. *Angew. Chem. Int. Ed.* **1999**, *38*, 166-168.
15. Arasasingham, R. D.; Balch, A. L.; Cornman, C. R.; Latos-Grazynski, L., Dioxygen insertion into iron(III)-carbon bonds. NMR studies of the formation and reactivity of alkylperoxo complexes of iron(III) porphyrins. *J. Am. Chem. Soc.* **1989**, *111*, 4357-4363.
16. Arasasingham, R. D.; Balch, A. L.; Latos-Grazynski, L., Identification of intermediates and products in the reaction of porphyrin iron(III) alkyl complexes with dioxygen. *J. Am. Chem. Soc.* **1987**, *109*, 5846-5847.
17. Sauer, A.; Cohen, H.; Meyerstein, D., Kinetics of the Homolytic Dioxygen Insertion into the Cobalt-Carbon Bond in (Nta)(H₂O)Co^{III}-CH₃-. *Inorg. Chem.* **1989**, *28*, 2511-2512.
18. Bakac, A.; Espenson, J. H., Reactions of Cobalt(II) Macrocycles with Alkyl and Alkylperoxy Radicals. *Inorg. Chem.* **1989**, *28*, 4319-4322.
19. Deniau, J.; Gaudemer, A., Stereochemical Study of the Reaction of Molecular-Oxygen with Alkylcobaloximes. *J. Organomet. Chem.* **1980**, *191*, C1-C2.
20. Rettenmeier, C. A.; Wadepohl, H.; Gade, L. H., Electronic structure and reactivity of nickel(I) pincer complexes: their aerobic transformation to peroxo species and site selective C-H oxygenation. *Chem. Sci.* **2016**, *7*, 3533-3542.

21. Mukherjee, D.; Ellern, A.; Sadow, A. D., Remarkably Robust Monomeric Alkylperoxyzinc Compounds from Tris(oxazolinyl)boratozinc Alkyls and O₂. *J. Am. Chem. Soc.* **2012**, *134*, 13018-13026.
22. Maury, J.; Feray, L.; Bazin, S.; Clement, J. L.; Marque, S. R.; Siri, D.; Bertrand, M. P., Spin-trapping evidence for the formation of alkyl, alkoxy, and alkylperoxy radicals in the reactions of dialkylzincs with oxygen. *Chem. Eur. J.* **2011**, *17*, 1586-1595.
23. Grice, K. A.; Goldberg, K. I., Insertion of Dioxygen into a Platinum(II)-Methyl Bond To Form a Platinum(II) Methylperoxo Complex. *Organometallics* **2009**, *28*, 953-955.
24. Boisvert, L.; Denney, M. C.; Hanson, S. K.; Goldberg, K. I., Insertion of molecular oxygen into a palladium(II) methyl bond: a radical chain mechanism involving palladium(III) intermediates. *J. Am. Chem. Soc.* **2009**, *131*, 15802-15814.
25. Taylor, R. A.; Law, D. J.; Sunley, G. J.; White, A. J. P.; Britovsek, G. J. P., Towards Photocatalytic Alkane Oxidation: The Insertion of Dioxygen into a Platinum(II)-Methyl Bond. *Angew. Chem. Int. Ed.* **2009**, *48*, 5900-5903.
26. Petersen, A. R.; Taylor, R. A.; Vicente-Hernandez, I.; Mallender, P. R.; Olley, H.; White, A. J.; Britovsek, G. J., Oxygen insertion into metal carbon bonds: formation of methylperoxo Pd(II) and Pt(II) complexes via photogenerated dinuclear intermediates. *J. Am. Chem. Soc.* **2014**, *136*, 14089-14099.
27. Petersen, A. R.; Taylor, R. A.; Vicente-Hernandez, I.; Heinzer, J.; White, A. J. P.; Britovsek, G. J. P., Light-Driven Methyl Exchange Reactions in Square-Planar Palladium(II) and Platinum(II) Complexes. *Organometallics* **2014**, *33*, 1453-1461.
28. Sicilia, V.; Baya, M.; Borja, P.; Martin, A., Oxidation of Half-Lantern Pt₂(II,II) Compounds by Halocarbons. Evidence of Dioxygen Insertion into a Pt(III)-CH₃ Bond. *Inorg. Chem.* **2015**, *54*, 7316-7324.
29. Khusnutdinova, J. R.; Rath, N. P.; Mirica, L. M., The aerobic oxidation of a Pd(II) dimethyl complex leads to selective ethane elimination from a Pd(III) intermediate. *J. Am. Chem. Soc.* **2012**, *134*, 2414-2422.
30. Powers, D. C.; Geibel, M. A.; Klein, J. E.; Ritter, T., Bimetallic palladium catalysis: direct observation of Pd(III)-Pd(III) intermediates. *J. Am. Chem. Soc.* **2009**, *131*, 17050-17051.
31. Powers, D. C.; Ritter, T., Bimetallic Pd(III) complexes in palladium-catalysed carbon-heteroatom bond formation. *Nat. Chem.* **2009**, *1*, 302-309.
32. Powers, D. C.; Xiao, D. Y.; Geibel, M. A.; Ritter, T., On the mechanism of palladium-catalyzed aromatic C-H oxidation. *J. Am. Chem. Soc.* **2010**, *132*, 14530-14536.
33. Elvidge, J. A.; Linsted, R. P., Conjugated Macrocycles. Part XXIV.* A New Type of Cross-conjugated Macrocyclic, related to the Azaporphins. *J. Chem. Soc.* **1952**, 5008-5012.
34. Wen, H. M.; Wang, J. Y.; Li, B.; Zhang, L. Y.; Chen, C. N.; Chen, Z. N., Phosphorescent square-planar platinum(II) complexes of 1,3-bis(2-pyridylimino)isoindoline with a monodentate strong-field ligand. *Eur. J. Inorg. Chem.* **2013**, 4789-4798.
35. Wen, H. M.; Wu, Y. H.; Fan, Y.; Zhang, L. Y.; Chen, C. N.; Chen, Z. N., Spectroscopic and luminescence studies on square-planar platinum(II) complexes with anionic tridentate 3-bis(2-pyridylimino)isoindoline derivatives. *Inorg. Chem.* **2010**, *49*, 2210-2221.
36. Hanson, K.; Roskop, L.; Patel, N.; Griffe, L.; Djurovich, P. I.; Gordon, M. S.; Thompson, M. E., Photophysical and electrochemical properties of 1,3-bis(2-pyridylimino)isoindolate platinum(ii) derivatives. *Dalton Trans.* **2012**, *41*, 8648-8659.
37. Siggelkow, B.; Meder, M. B.; Galka, C. H.; Gade, L. H., Synthesis, Structures and Catalytic Properties of Bis(2-pyridylimino)-isoindolatopalladium Complexes. *Eur. J. Inorg. Chem.* **2004**, *2004*, 3424-3435.

38. Zeitler, H. E.; Kaminsky, W. A.; Goldberg, K. I., Insertion of Molecular Oxygen into the Metal–Methyl Bonds of Platinum(II) and Palladium(II) 1,3-Bis(2-pyridylimino)isoindolate Complexes. *Organometallics* **2018**, *37*, 3644-3648.
39. Chavez, F. A.; Mascharak, P. K., Co(III) - Alkylperoxo complexes: Syntheses, structure - Reactivity correlations, and use in the oxidation of hydrocarbons. *Acc. Chem. Res.* **2000**, *33*, 539-545.
40. Farinas, E. T.; Nguyen, C. V.; Mascharak, P. K., Photoinduced oxidation of hydrocarbons with cobalt(III)-alkylperoxy complexes. *Inorg. Chim. Acta* **1997**, *263*, 17-21.
41. Saussine, L.; Brazi, E.; Robine, A.; Mimoun, H.; Fischer, J.; Weiss, R., Cobalt(III) Alkylperoxy Complexes. Synthesis, X-ray Structure, and Role in the Catalytic Decomposition of Alkyl Hydroperoxides and in the Hydroxylation of Hydrocarbons. *J. Am. Chem. Soc.* **1985**, *107*, 3534-3540.
42. Rettenmeier, C. A.; Wadepohl, H.; Gade, L. H., Electronic structure and reactivity of nickel(i) pincer complexes: Their aerobic transformation to peroxo species and site selective C-H oxygenation. *Chem. Sci.* **2016**, *7*, 3533-3542.
43. Hoffmann, N., Homogeneous Photocatalytic Reactions with Organometallic and Coordination Compounds—Perspectives for Sustainable Chemistry. *ChemSusChem* **2012**, *5*, 352-371.
44. Hanson, K.; Roskop, L.; Patel, N.; Griffe, L.; Djurovich, P. I.; Gordon, M. S.; Thompson, M. E., Photophysical and electrochemical properties of 1,3-bis(2-pyridylimino)isoindolate platinum(II) derivatives. *Dalton Trans.* **2012**, *41*, 8648-8659.
45. Wen, H. M.; Wu, Y. H.; Xu, L. J.; Zhang, L. Y.; Chen, C. N.; Chen, Z. N., Luminescent square-planar platinum(II) complexes with tridentate 3-bis(2-pyridylimino)isoindoline and monodentate N-heterocyclic ligands. *Dalton Trans.* **2011**, *40*, 6929-6938.
46. Ortuno, M. A.; Conejero, S.; Lledos, A., True and masked three-coordinate T-shaped platinum(II) intermediates. *Beilstein J. Org. Chem.* **2013**, *9*, 1352-1382.
47. Fafard, C. M.; Adhikari, D.; Foxman, B. M.; Mindiola, D. J.; Ozerov, O. V., Addition of ammonia, water, and dihydrogen across a single Pd-Pd bond. *J. Am. Chem. Soc.* **2007**, *129*, 10318-10319.
48. Aye, K.-T.; Canty, A. J.; Crespo, M.; Puddephatt, R. J.; Scott, J. D.; Watson, A. A., Alkyl halide transfer from palladium(IV) to platinum(II) and a study of reactivity, selectivity, and mechanism in this and related reactions. *Organometallics* **1989**, *8*, 1518-1522.
49. Ananikov, V. P.; Musaev, D. G.; Morokuma, K., Theoretical insight into the C-C coupling reactions of the vinyl, phenyl, ethynyl, and methyl complexes of palladium and platinum. *Organometallics* **2005**, *24*, 715-723.
50. Hackett, M.; Whitesides, G. M., Bis(cyclohexylphosphino)ethane)platinum(0). Reactions with alkyl, TMSmethyl, aryl, benzyl and alkynyl carbon-hydrogen bonds. *J. Am. Chem. Soc.* **1988**, *110*, 1449-1462.
51. Hill, G. S.; Puddephatt, R. J., Electrophilic Methylplatinum Complexes: A Theoretical Study of the Mechanism of C–C and C–H Bond Formation and Activation. *Organometallics* **1998**, *17*, 1478-1486.
52. Bryndza, H. E.; Fong, L. K.; Paciello, R. A.; Tam, W.; Bercaw, J. E., Relative Metal-hydrogen Bond Strengths. *J. Am. Chem. Soc.* **1987**, *109*, 1444-1456.
53. Jiao, Y.; Evans, M. E.; Morris, J.; Brennessel, W. W.; Jones, W. D., Rhodium-carbon bond energies in Tp'Rh(CNneopentyl)(CH₂X)H: quantifying stabilization effects in M-C bonds. *J. Am. Chem. Soc.* **2013**, *135*, 6994-7004.
54. Siegbahn, P. E. M., Trends of Metal-Carbon Bond Strengths in Transition Metal Complexes. *J. Phys. Chem.* **1995**, *99*, 12723-12729.
55. Van Leeuwen, P. W. N. M.; Roobeek, C. F.; Huis, R., Photodecomposition of platinum and palladium alkyls: A cidnp study. *J. Organomet. Chem.* **1977**, *142*, 233-241.
56. Klein, A.; van Slageren, J.; Zalis, S., Spectroscopy and photochemical reactivity of cyclooctadiene platinum complexes. *J. Organomet. Chem.* **2001**, *620*, 202-210.

57. Anklanlec, B. C.; Hardy, D. T.; Thomson, S. K.; Watkins, W. N.; Young, G. B., Mechanistic Studies of the Thermolytic and Photolytic Rearrangement of [Bis(diphenylphosphino)ethane]bis(neophyl)platinum(II). *Organometallics* **1992**, *11*, 2591-2598.
58. Burns, C. T.; Shen, H.; Jordan, R. F., Photochemical synthesis of a palladium dichloromethyl complex, $\{(\text{hexyl})\text{HC}(\text{N-methyl-imidazol-2-yl})_2\}\text{Pd}(\text{CHCl}(\text{2}))\text{Cl}$. X-ray molecular structures of $\{(\text{hexyl})\text{HC}(\text{N-methylimidazolyl-2-yl})(\text{2})\}\text{Pd}(\text{X})\text{Cl}$, $\text{X}=\text{C1}$, and $\text{CHCl}(\text{2})$. *J. Organomet. Chem.* **2003**, *683*, 240-248.
59. Alt, H. G., Photochemistry of Alkyltransition-Metal Complexes. *Angew. Chem. Int. Ed. Engl.* **1984**, *23*, 766-782.
60. Abo-Amer, A.; McCready, M. S.; Zhang, F.; Puddephatt, R. J., The role of solvent in organometallic chemistry — Oxidative addition with dichloromethane or chloroform. *Can. J. Chem.* **2011**, *90*, 46-54.
61. Alapi, T.; Dombi, A., Direct VUV photolysis of chlorinated methanes and their mixtures in an oxygen stream using an ozone producing low-pressure mercury vapour lamp. *Chemosphere* **2007**, *67*, 693-701.
62. Kuwahara, Y.; Zhang, A.; Soma, H.; Tsuda, A., Photochemical Molecular Storage of Cl_2 , HCl , and COCl_2 : Synthesis of Organochlorine Compounds, Salts, Ureas, and Polycarbonate with Photodecomposed Chloroform. *Org. Lett.* **2012**, *14*, 3376-3379.
63. Lee, B.-K.; Yoon, J. H.; Yoon, S.; Cho, B.-K., Induced Eye-detectable Blue Emission of Triazolyl Derivatives via Selective Photodecomposition of Chloroform under UV Irradiation at 365 nm. *Bull. Korean Chem. Soc.* **2014**, *35*, 135-140.
64. Muñoz, Z.; Cohen, A. S.; Nguyen, L. M.; McIntosh, T. A.; Hoggard, P. E., Photocatalysis by tetraphenylporphyrin of the decomposition of chloroform. *Photochem. & Photobio. Sci.* **2008**, *7*, 337-343.
65. Rendina, L. M.; Puddephatt, R. J., Oxidative Addition Reactions of Organoplatinum(II) Complexes with Nitrogen-Donor Ligands. *Chem. Rev.* **1997**, *97*, 1735-1754.
66. Anderson, O. P.; la Cour, A.; Berg, A.; Garrett, A. D.; Wicholas, M., Fluxional Behavior of a Cadmium Zwitterion Complex: Proton Transport and Tautomerism in Methylene Chloride Solution. *Inorg. Chem.* **2003**, *42*, 4513-4515.
67. Zeitler, H. E.; Kaminsky, W. A.; Goldberg, K. I., Insertion of Molecular Oxygen into the Metal-Methyl Bonds of Platinum(II) and Palladium(II) 1,3-Bis(2-pyridylimino)isoindolate Complexes. *Organometallics* **2018**, *37*, 3644-3648.
68. Miyaji, T.; Kujime, M.; Hikichi, S.; Moro-oka, Y.; Akita, M., Synthesis and Characterization of a Series of (Hydroperoxo)-, (Alkylperoxo)-, and (μ -Peroxo)palladium Complexes Containing the Hydrotris(3,5-diisopropylpyrazolyl)borato Ligand (TpiPr₂): (TpiPr₂)(py)Pd-OO-X [X = H, t-Bu, Pd(TpiPr₂)(py)] and (TpiPr₂)(py)Pd-(μ - κ 1: κ 2-OO)-PdTpiPr₂. *Inorg. Chem.* **2002**, *41*, 5286-5295.
69. Yang, Y.; Zhang, D.; Wu, L. Z.; Chen, B.; Zhang, L. P.; Tung, C. H., Photosensitized oxidative deprotection of oximes to their corresponding carbonyl compounds by platinum(II) terpyridyl acetylide complex. *J. Org. Chem.* **2004**, *69*, 4788-4791.
70. Lengfelder, E.; Cadenas, E.; Sies, H., Effect of DABCO (1,4-diazabicyclo[2,2,2]-octane) on singlet oxygen monomol (1270 nm) and dimol (634 and 703 nm) emission. *FEBS Lett.* **1983**, *164*, 366-370.
71. Zhang, Y.; Ley, K. D.; Schanze, K. S., Photooxidation of Diimine Dithiolate Platinum(II) Complexes Induced by Charge Transfer to Diimine Excitation. *Inorg. Chem.* **1996**, *35*, 7102-7110.
72. Craig, P. J.; Green, M., Carbonyl Insertion Reactions of Methyl- and Ethyl-tricarbonylcyclopentadienylmolybdenum. *J. Chem. Soc. A* **1968**, 1978-1981.

73. Vaska, L., Dioxygen-Metal Complexes - Toward A Unified View. *Acc. Chem. Res.* **1976**, *9*, 175-183.
74. Kashiwagi, T.; Yasuoka, N.; Kasai, N.; Kakudo, M.; Takahashi, S.; Hagihara, N., Crystal and molecular structure of the oxygen adduct, $[\text{Pt}(\text{O}_2)(\text{PPh}_3)_2] \cdot 1.5 \text{C}_6\text{H}_6$. *J. Chem. Soc. D: Chem. Commun.* **1969**, 743-743.
75. Muto, S.; Kamiya, Y., Reaction of Carboxylic Acids with Dioxygen Complexes: A Mechanistic Aspect of the Reaction. *Bull. Chem. Soc. Jpn.* **1976**, *49*, 2587-2589.
76. Haarman, H. F.; Bregman, F. R.; van Leeuwen, P. W. N. M.; Vrieze, K., Reaction of a Rhodium(III) α -Chlorotolyl Complex with Water and Oxygen: Stable Rhodium Peroxo Compounds. *Organometallics* **1997**, *16*, 979-985.
77. Sieh, D.; Schlimm, M.; Andernach, L.; Angersbach, F.; Nüchel, S.; Schöffel, J.; Šušnjar, N.; Burger, P., Metal-Ligand Electron Transfer in 4d and 5d Group 9 Transition Metal Complexes with Pyridine, Diimine Ligands. *Eur. J. Inorg. Chem.* **2012**, *2012*, 444-462.
78. Penner, A.; Schröder, T.; Braun, T.; Ziemer, B., Synthesis, Structure, and Reactivity of Rhodium Bipyridine Compounds: Formation of a RhII Hydrido Cluster and a RhIII Peroxido Complex. *Eur. J. Inorg. Chem.* **2009**, *2009*, 4464-4470.
79. de Bruin, B.; Peters, Theo P. J.; Wilting, Jos B. M.; Thewissen, S.; Smits, Jan M. M.; Gal, Anton W., Dioxygenation of Sterically Hindered (Ethene)RhI and -IrI Complexes to (Peroxo)RhIII and (Ethene)(peroxo)IrIII Complexes. *Eur. J. Inorg. Chem.* **2002**, *2002*, 2671-2680.
80. Polukeev, A. V.; Wendt, O. F., Iridium Pincer Complexes with an Olefin Backbone. *Organometallics* **2015**, *34*, 4262-4271.
81. Feller, M.; Ben-Ari, E.; Diskin-Posner, Y.; Carmieli, R.; Weiner, L.; Milstein, D., O_2 activation by metal-ligand cooperation with Ir(I) PNP pincer complexes. *J. Am. Chem. Soc.* **2015**, *137*, 4634-4637.
82. Hoseini, S. J.; Fath, R. H.; Fard, M. A.; Behnia, A.; Puddephatt, R. J., A Bridging Peroxide Complex of Platinum(IV). *Inorg. Chem.* **2018**, *57*, 8951-8955.
83. Qu, F.; Khusnutdinova, J. R.; Rath, N. P.; Mirica, L. M., Dioxygen activation by an organometallic Pd(II) precursor: formation of a Pd(IV)-OH complex and its C-O bond formation reactivity. *Chem. Commun.* **2014**, *50*, 3036-3039.
84. Liu, W.-G.; Sberegaeva, A. V.; Nielsen, R. J.; Goddard, W. A.; Vedernikov, A. N., Mechanism of O_2 Activation and Methanol Production by (Di(2-pyridyl)methanesulfonate)PtII $\text{Me}(\text{OH})_{(2-n)}$ -Complex from Theory with Validation from Experiment. *J. Amer. Chem. Soc.* **2014**, *136*, 2335-2341.
85. Davies, M. S.; Hambley, T. W., $[\text{Pt}_2\text{Cl}_2(\mu_2\text{-O}_2)_2([\text{9}]\text{aneN}_3)_2]\text{Cl}_2$: A Novel Platinum(IV) Dimer with Two Bridging Peroxo Ligands that Provides Insight into the Mechanism of Aerial Oxidation of Platinum(II). *Inorg. Chem.* **1998**, *37*, 5408-5409.
86. Kornblum, N.; DeLaMare, H. E., The Base Catalyzed Decomposition Of A Dialkyl Peroxide. *J. Am. Chem. Soc.* **1951**, *73*, 880-881.
87. Walling, C.; Buckler, S. A., The Reaction of Oxygen with Organometallic Compounds. A New Synthesis of Hydroperoxides. *J. Am. Chem. Soc.* **1955**, *77*, 6032-6038.
88. Al-Shihri, S.; Richard, C. J.; Chadwick, D., Selective Oxidation of Methane to Methanol over ZSM-5 Catalysts in Aqueous Hydrogen Peroxide: Role of Formaldehyde. *ChemCatChem* **2017**, *9*, 1276-1283.
89. Matthews, J.; Sinha, A.; Francisco, J. S., Unimolecular dissociation and thermochemistry of CH_3OOH . *J. Chem. Phys.* **2005**, *122*, 221101.
90. Phillips, D. L.; Zhao, C.; Wang, D., A theoretical study of the mechanism of the water-catalyzed HCl elimination reactions of $\text{CHXCl}(\text{OH})$ ($\text{X} = \text{H}, \text{Cl}$) and HClCO in the gas phase and in aqueous solution. *J. Phys. Chem. A* **2005**, *109*, 9653-9673.

91. Puddephatt, R. J.; Scott, J. D., Oxidative addition to methylplatinum(II) complexes: trapping of a cationic intermediate and a comparison of reactivities of mononuclear and binuclear complexes. *Organometallics* **1985**, *4*, 1221-1223.
92. Hux, J. E.; Puddephatt, R. J., Photochemistry of Mononuclear and Binuclear Tetramethylplatinum(IV) Complexes - Reactivity of an Organometallic Free-Radical. *J. Organomet. Chem.* **1992**, *437*, 251-263.
93. Scheuermann, M. L.; Luedtke, A. T.; Hanson, S. K.; Fekl, U.; Kaminsky, W.; Goldberg, K. I., Reactions of Five-Coordinate Platinum(IV) Complexes with Molecular Oxygen. *Organometallics* **2013**, *32*, 4752-4758.
94. Look, J. L.; Wick, D. D.; Mayer, J. M.; Goldberg, K. I., Autoxidation of Platinum(IV) Hydrocarbyl Hydride Complexes To Form Platinum(IV) Hydrocarbyl Hydroperoxide Complexes. *Inorg. Chem.* **2009**, *48*, 1356-1369.
95. Motiyenko, R. A.; Margulès, L.; Despois, D.; Guillemin, J.-C., Laboratory spectroscopy of methoxymethanol in the millimeter-wave range. *Phys. Chem. Chem. Phys.* **2018**, *20*, 5509-5516.
96. Citir, M.; Metz, R. B.; Belau, L.; Ahmed, M., Direct determination of the ionization energies of PtC, PtO, and PtO₂ with VUV radiation. *J. Phys. Chem. A* **2008**, *112*, 9584-9590.
97. Denney, M. C.; Smythe, N. A.; Cetto, K. L.; Kemp, R. A.; Goldberg, K. I., Insertion of Molecular Oxygen into a Palladium(II) Hydride Bond. *J. Am. Chem. Soc.* **2006**, *128*, 2508-2509.
98. Konnick, M. M.; Stahl, S. S., Reaction of molecular oxygen with a Pd(II)-hydride to produce a Pd(II)-hydroperoxide: experimental evidence for an HX-reductive-elimination pathway. *J. Am. Chem. Soc.* **2008**, *130*, 5753-5762.
99. Szajna-Fuller, E.; Bakac, A., Base-Catalyzed Insertion of Dioxygen into Rhodium-Hydrogen Bonds: Kinetics and Mechanism. *Inorg. Chem.* **2010**, *49*, 781-785.
100. Decharin, N.; Popp, B. V.; Stahl, S. S., Reaction of O₂ with (-)-Sparteine Pd(H)Cl: Evidence for an Intramolecular H-L (+) "Reductive Elimination" Pathway. *J. Am. Chem. Soc.* **2011**, *133*, 13268-13271.
101. Konnick, M. M.; Decharin, N.; Popp, B. V.; Stahl, S. S., O₂ insertion into a palladium(II)-hydride bond: Observation of mechanistic crossover between HX-reductive-elimination and hydrogen-atom-abstraction pathways. *Chem. Sci.* **2011**, *2*, 326-330.
102. Keith, J. M.; Muller, R. P.; Kemp, R. A.; Goldberg, K. I.; Goddard, W. A.; Oxgaard, J., Mechanism of Direct Molecular Oxygen Insertion in a Palladium(II)-Hydride Bond. *Inorg. Chem.* **2006**, *45*, 9631-9633.
103. Keith, J. M.; Goddard, W. A.; Oxgaard, J., Pd-Mediated Activation of Molecular Oxygen: Pd(0) versus Direct Insertion. *J. Am. Chem. Soc.* **2007**, *129*, 10361-10369.
104. Han, R.; Parkin, G., Tris(Pyrazolyl)Hydroborato Magnesium Alkyl Derivatives - Reactivity Studies. *J. Am. Chem. Soc.* **1992**, *114*, 748-757.
105. Poli, R.; Harvey, J. N., Spin forbidden chemical reactions of transition metal compounds. New ideas and new computational challenges. *Chem. Soc. Rev.* **2003**, *32*, 1-8.
106. Fernández-Alvarez, V. M.; Ho, S. K. Y.; Britovsek, G. J. P.; Maseras, F., A DFT-based mechanistic proposal for the light-driven insertion of dioxygen into Pt(II)-C bonds. *Chem. Sci.* **2018**, *9*, 5039-5046.
107. Álvarez-Moreno, M.; de Graaf, C.; López, N.; Maseras, F.; Poblet, J. M.; Bo, C., Managing the Computational Chemistry Big Data Problem: The ioChem-BD Platform. *J. Chem. Inform. Mod.* **2015**, *55*, 95-103.
108. Sousa, D. W. O. d.; Nascimento, M. A. C., Are One-Electron Bonds Any Different from Standard Two-Electron Covalent Bonds? *Acc. Chem. Res.* **2017**, *50*, 2264-2272.

109. Moret, M.-E.; Zhang, L.; Peters, J. C., A Polar Copper–Boron One-Electron σ -Bond. *J. Amer. Chem. Soc.* **2013**, *135*, 3792-3795.
110. Sehnal, P.; Taylor, R. J. K.; Fairlamb, I. J. S., Emergence of Palladium(IV) Chemistry in Synthesis and Catalysis. *Chem. Rev.* **2010**, *110*, 824-889.
111. Xu, L.-M.; Li, B.-J.; Yang, Z.; Shi, Z.-J., Organopalladium(IV) chemistry. *Chem. Soc. Rev.* **2010**, *39*, 712-733.

For Table of Contents Only:

